UNIVERSITY OF TURKU

NRG1/ERBB Axis in Drug Tolerance to Targeted Cancer Therapies

Institute of Biomedicine
MDP in Biomedical Sciences, Drug Discovery and Development
Master's thesis

Author:
Sara Peltola

Supervisor:
Docent Kari Kurppa, Institute of Biomedicine, University of Turku

25.4.2024
Turku

Master's thesis

Subject: Institute of Biomedicine, MDP in Biomedical Sciences, Drug Discovery and Development
Author: Sara Peltola
Title: NRG1/ERBB Axis in Drug Tolerance to Targeted Cancer Therapies
Supervisor: Docent Kari Kurppa, University of Turku
Number of pages and Appendices: 70 pages, 3 appendices
Date: 25.4.2024

Targeted therapies have benefited many patients, but resistance significantly hinders the long-term efficacy of these treatments. Development of resistance is complex and can occur through various mechanisms including involvement of drug-tolerant persister cells. These nonproliferating cells can survive under drug exposure by nongenetic mechanisms and, over time, acquire mutations that confer therapy resistance.

The erythroblastic leukemia viral oncogene homolog (ERBB) receptor family including epidermal growth factor receptor (EGFR), ERBB2, ERBB3 and ERBB4 is linked to many cancers. Exogenous neuregulin 1 (NRG1), a ligand of ERBB3 and ERBB4, strongly promotes resistance to targeted therapy in oncogene-addicted cancer cell lines. Additionally, previous data from our group show an upregulation of NRGs and their receptors in drug-tolerant cells.

The main goal of this thesis was to determine the functional relevance of upregulation of NRGs and their receptors in drug-tolerant cells. The first aim was to investigate whether the upregulation of NRGs and their receptors result in elevated activation of the ERBB receptors, which was analyzed by western blotting in five cancer cell lines treated with targeted therapies for up to 30 days. The second aim was to study the necessity of ERBB receptors to the drug-tolerant cells by CRISPR-Cas9-mediated knockout.

The most prominent reactivation of the ERBB signaling was observed in *ALK*-rearranged adenocarcinoma and *BRAF*-mutated colorectal cancer cell lines H3122 and HT-29, respectively. The knockout studies further implicate the importance of EGFR, ERBB2 and ERBB3 to drug-tolerant H3122 cells and ERBB2 to drug-tolerant HT-29 cells. In future studies it would be meaningful to investigate whether blocking of these receptors by an antibody upon the original targeted therapy treatment decreases cancer cell viability, which would suggest the potential of the treatment combination in the clinic.

Key words: cancer, drug-tolerant persister cells, ERBB receptor, NRG

Table of contents

1 Introduction 6

1.1 Global burden of cancer 6

1.2 Targeted therapies in treatment of oncogene-addicted cancers 6

1.2.1 Oncogene addiction 6

1.2.2 Kinase inhibitors as a class of targeted therapies 7

1.3 ERBB receptor family and its significance in cancer 8

1.3.1 ERBB structure and signaling 8

1.3.2 ERBB ligands 10

1.3.3 ERBBs as oncogenic drivers 11

1.4 Resistance to targeted cancer therapies 12

1.4.1 Scope of the issue 12

1.4.2 Different types of kinase inhibitor resistance mechanisms 12

1.4.3 Primary and acquired resistance 13

1.4.4 NRG1/ERBB axis in drug resistance 14

1.5 CRISPR-Cas9 as a tool for gene knockout studies 15

1.6 Aims and hypotheses 16

1.6.1 Aims 16

1.6.2 Hypotheses 17

2 Results 18

2.1 Activation of ERBB signaling in oncogene-addicted cancer cell lines upon SOC targeted treatment 18

2.1.1 Robust reactivation of ERBB signaling upon 10-day SOC targeted treatment in H3122 and HT-29 cells 18

2.1.2 ERBB receptor reactivation upon SOC targeted treatment peaks at 10 to 20 days in H3122 and HT-29 cells 22

2.2 Necessity of NRG/ERBB signaling for survival of drug-tolerant cells 27

2.2.1 Selection of best gRNAs for knocking out *ERBBs* using CRISPR-Cas9 27

2.2.2 CRISPR efficiency in H3122 and HT-29 cells 30

2.2.3 Dependency of H3122 cells on EGFR, ERBB2, and ERBB3, and ERBB2 dependency in HT-29 cells 31

3 Discussion 37

3.1 Significance of NRG/ERBB signaling to drug tolerance in different oncogene-addicted cancer contexts 38

3.1.1 *HER2*-amplified breast cancer 38

3.1.2 *EGFR*-mutated NSCLC 39
3.1.3 *BRAF* V600E -mutated melanoma 40
3.1.4 *ALK*-positive NSCLC 41
3.1.5 *BRAF* V600E -mutated colorectal cancer 43

3.2 Possible sources of error and study limitations 44
3.2.1 ERBB signaling activation experiments 44
3.2.2 ERBB receptor dependency experiments 45

3.3 Conclusion and future directions 46

4 Materials and methods 47

4.1 Cell culture 47

4.2 *ERBB* knockouts using CRISPR and nucleofection 47
4.2.1 RNP complex assembly 47
4.2.2 Nucleofection 48
4.2.3 Post-nucleofection 48

4.3 10- and 30-day drug treatments with SOC targeted therapies 49
4.3.1 10-day treatment of wild-type oncogene-addicted cancer cells 49
4.3.2 30-day treatment of wild-type oncogene-addicted cancer cells 51
4.3.3 10-day treatment of ERBB receptor knockout cell pools 52

4.4 Western blot 53
4.4.1 Sample preparation 53
4.4.2 SDS-page 54
4.4.3 Protein transfer, blocking and imaging of the membranes 54
4.4.4 Stripping 56

4.5 Sample preparation for Next-generation sequencing 56
4.5.1 DNA extraction 56
4.5.2 PCR and agarose gel electrophoresis 56

4.6 Data analysis 58

5 Acknowledgements 59

6 List of abbreviations 60

References 61

Appendices 71

Appendix 1 - Preparation of buffers for western blotting 71
Lysis buffer 71
6x SDS sample buffer 71

10x Western buffer 71
Running buffer 72
Transfer buffer 72
Stripping buffer 72
10x TBST 72
Appendix 2 - crRNA sequences **73**
Appendix 3 - PCR primer sequences **73**

1 Introduction

1.1 Global burden of cancer

Cancer is not one but a collection of over 100 distinct diseases that are characterized by uncontrolled cell proliferation, invasion of nearby tissues and development of distant metastases (Stratton et al., 2009). Cancer creates an enormous global health burden with incidence of 19.3 million and 10 million caused deaths in 2020 according to GLOBOCAN estimates (Sung et al., 2021). The World Health Organization has estimated cancer to be either the second or first most common cause of death in under 70-year-old individuals in 61 % of the 183 evaluated countries (World Health Organization (WHO), 2020). The incidence of cancer is expected to rise by 47 % in the next 20 years (Sung et al., 2021).

1.2 Targeted therapies in treatment of oncogene-addicted cancers

1.2.1 Oncogene addiction

Cancer often results from oncogenic alterations in genes, which encode cell signaling proteins controlling cell proliferation, such as protein tyrosine kinases (PTKs) (Yang et al., 2022). These genetic alterations include gene amplifications, gene fusions, single-nucleotide variants and indels referring to short deletions and insertions of nucleotides (Martínez-Jiménez et al., 2020). Gene amplification can be defined as overexpression of a gene caused by somatic rise in copy number of a genomic region (Santarius et al., 2010). Gene fusions, in contrast, result from structural rearrangements in chromosomes, where regulatory or coding sequences from two genes are fused together. This can occur through exchange of DNA segments between two chromosomes, insertions or deletions of chromosome segments or inversions within a chromosome (Mertens et al., 2015). Interestingly, cancer cells are often dependent on one single overexpressed or mutated oncogene to remain tumorigenic. This dependence is referred to as oncogene addiction (Weinstein, 2002).

Examples of oncogene addiction include, for instance, activating mutations in *BRAF* encoding serine/threonine protein kinase part of the RAS/RAF/Mitogen-activated protein kinase/ERK kinase (MEK)/extracellular-signal-regulated kinase (ERK) signaling pathway. Half of melanoma patients present activating *BRAF* mutations of which V600E point mutation, where valine is replaced by glutamic acid, is the most frequent (Ascierto et al., 2012). Besides melanoma, *BRAF* V600E mutation is also seen in around 10 % of patients with metastatic colorectal cancer (Morris et al., 2014).

Another well-known example of oncogene addiction is the fusion tyrosine kinase between echinoderm microtubule-associated protein-like 4 (EML4) and anaplastic lymphoma kinase (ALK). This EML4-ALK fusion kinase results from inversion within the short arm of chromosome two. The kinase is constitutively active and presents oncogenic transformation potential both *in vitro* and *in vivo* (Soda et al., 2007). The fusion gene has been reported in lung cancer and is shown to be specific to adenocarcinomas, being present in 3.4 % of the cases (Inamura et al., 2008).

Additionally, amplification of gene encoding hepatocyte growth factor receptor, *MET*, locally in chromosome 7q31 is seen in non-small-cell lung cancer (NSCLC) as de novo oncogenic alteration driving the tumor growth in 1-5 % of the cases (Remon et al., 2023). Although rare, *MET* amplifications serve as a marker for poor prognosis in NSCLC patients, who have received surgery as treatment for their cancer (Cappuzzo et al., 2009).

1.2.2 Kinase inhibitors as a class of targeted therapies

Currently, many oncogene-addicted cancers can be treated with drugs that inhibit the action of an oncogene with high specificity. These treatments are referred to as targeted therapies. For instance, overexpressed and mutated kinases can be targeted with small-molecule kinase inhibitors, which are one of the most common classes of targeted therapies used in treating cancer (Yang et al., 2022). Kinase inhibitors are divided into two classes based on their binding mode, namely reversible and irreversible inhibitors. Reversible kinase inhibitors are further divided into four types depending on the region they bind to on their target and whether they bind active or inactive kinases. Type I kinase inhibitors bind to ATP-binding site on an active kinase. In contrast, type II kinase inhibitors bind to an inactive kinase stabilizing it. Type III and IV kinase inhibitors bind to allosteric sites either neighboring or distant to the ATP-binding site, respectively (Wu et al., 2015). Nevertheless, all kinase inhibitors block downstream signaling from their target kinase by inhibiting the ability of the kinase to phosphorylate its protein substrate by transferring phosphate groups from ATP to the substrate (Huang et al., 2020). High efficiency and specificity as well as low toxicity give kinase inhibitors a great advantage over traditionally used chemotherapeutic regimens (Yang et al., 2022).

The aforementioned *EML4-ALK*-positive and *MET*-amplified cancers can be treated with a kinase inhibitor crizotinib, which is a dual inhibitor targeting ALK and MET (O'Bryant et al., 2013). The oncogenic *BRAF* V600E, in contrast, can be targeted with kinase inhibitors vemurafenib or dabrafenib (Ascierto et al., 2012). Dabrafenib is used in combination with MEK inhibitor trametinib in treatment of most solid cancers as the combination treatment has demonstrated good response in several cancer types (Bouffet et al., 2023; Planchard et al., 2016; Subbiah et al., 2020, 2022). In addition, the combination treatment has shown to hinder development of resistance and to demonstrate better tolerability in melanoma harboring *BRAF* V600E mutation compared to dabrafenib as a single agent (Long et al., 2014). In treatment of colorectal cancer, however, dabrafenib is often combined with a monoclonal anti-epidermal growth factor receptor (EGFR) antibody cetuximab. The patients benefit from this combination treatment, since upon BRAF inhibition in colorectal cancer, EGFR becomes activated through a feedback loop and promotes cancer cell proliferation (Prahallad et al., 2012).

1.3 ERBB receptor family and its significance in cancer

1.3.1 ERBB structure and signaling

PTKs are divided into non-receptor tyrosine kinases (NRTKs) and receptor tyrosine kinases (RTKs) (Yang et al., 2022). Erythroblastic leukemia viral oncogene homolog (ERBB) receptor family consisting of EGFR, ERBB2 (human epidermal growth factor receptor 2 (HER2)), ERBB3 (HER3) and ERBB4 (HER4) belongs to RTKs (Arteaga & Engelman, 2014). In physiological context, ERBB signaling is crucial for organogenesis including the development of heart and nervous system (Burden & Yarden, 1997b).

The ERBB receptors contain an extracellular region for ligand-binding, a transmembrane domain, and a cytoplasmic tyrosine kinase domain located between an intracellular juxtamembrane region and C-terminal tail (Burgess et al., 2003). The extracellular region is further divided into four subdomains, namely I, II, III and IV (Lax et al., 1988). The ERBB ligands bind between the subdomains I and III forming interactions with both subdomains (Burgess et al., 2003). The subdomain II, on the other hand, contains a dimerization arm required for forming dimers by the monomeric receptors (Ogiso et al., 2002).

The ERBB receptors can adopt two configurations: tethered and exposed. In the tethered configuration the dimerization arm of subdomain II is hidden, which prevents receptor dimerization. Moreover, the distance between subdomains I and III is too long for a ligand to bind between them. All ERBB receptors exist in the tethered configuration as monomers except ERBB2, which is constantly in extended form. Upon ligand binding the tethered configuration becomes extended bringing subdomains I and III closer together and exposing subdomain II for dimerization (Burgess et al., 2003).

The dimerized receptors become activated by auto-phosphorylation of the tyrosine residues in the C-terminal tail occurring in *trans* meaning that the monomeric receptors forming the dimer phosphorylate each other (**Figure 1**). The ERBBs can form both homodimers and heterodimers of which ERBB1/ERBB2, ERBB2/ERBB3 and ERBB2/ERBB4 are most common (Segers et al., 2020). Interestingly, ERBB3 does not elicit kinase activity but uses heterodimerization with other ERBB receptors for signaling. Generally, heterodimers are more potent in promoting cell proliferation compared to homodimers. ERBB2 is the preferred dimerization partner for the other ERBB receptors as it can form more stable dimers due to its slower rate of internalization compared to EGFR and slow ligand dissociation rate observed in heterodimers. Existing constantly in the exposed conformation also allows ERBB2 to be more ready to form dimers with the other ERBBs. The ERBB2/ERBB3 complex is the most potent of the heterodimers whereas the least potent and stable is the ERBB3/ERBB4 dimer (Breuleux, 2007; Burden & Yarden, 1997a). The ERBB receptor phosphorylation leads to activation of downstream pathways, such as RAS/RAF/MEK/ERK and phosphoinositide 3-kinase (PI3K)/AKT signaling pathways, which promote cell division and inhibit apoptosis (Yarden & Pines, 2012; Yarden & Sliwkowski, 2001).

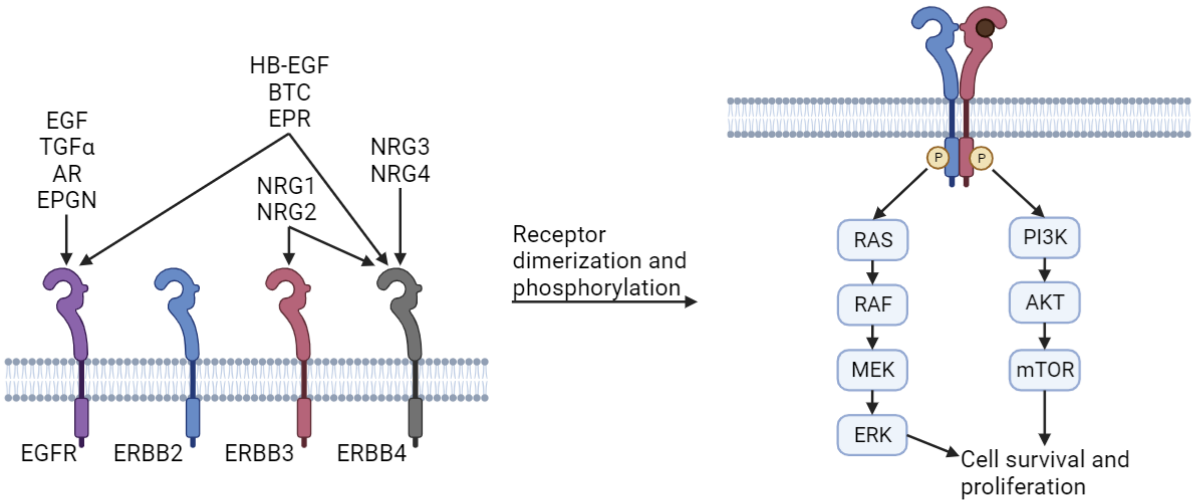

Figure 1. Simplified illustration of the ERBB signaling. The ligands for each ERBB receptor are indicated in the figure. Ligand binding triggers receptor dimerization and auto-phosphorylation. The activated receptor dimers activate multiple downstream signaling pathways including the RAS/RAF/MEK/ERK and PI3K/AKT pathways. AR = amphiregulin, EPGN = epigen, BTC = betacellulin, EPR = epiregulin. The figure was created in BioRender.com by the author.

1.3.2 ERBB ligands

All ligands of ERBB receptors belong to the EGF family and contain an EGF-like domain used to bind and activate the ERBB receptors (Breuleux, 2007). The domain contains six cysteine residues, which are spatially conserved between the ligands and form three disulfide bridges within the domain. The ERBB ligands are synthesized as membrane-bound precursors, which release the active ligand from the cell membrane by proteolytic cleavage (Lemmon et al., 2014). The active ligands can then signal either in autocrine or paracrine fashion (Breuleux, 2007). Additionally, juxtacrine signaling has been reported with intact membrane-bound ligands interacting with the ERBB receptors (Montero et al., 2007; Yang et al., 2000).

While EGFR and ERBB4 have the highest number of identified ligands, ERBB2 does not have any high affinity ligands. EGFR binds EGF, transforming growth factor α (TGF-α), amphiregulin, epigen, heparin-binding EGF-like growth factor (HB-EGF), betacellulin and epiregulin, of which the three last ones also bind ERBB4. Additionally, ERBB4 as well as ERBB3 act as receptors for neuregulins (NRGs), which consist of four members. NRG3 and NRG4 can only bind to ERBB4 but NRG1 and NRG2 are ligands for both ERBB3 and ERBB4 (Yarden & Pines, 2012). In addition to the four NRG members, alternative splicing creates over 20 NRG isoforms (Montero et al., 2008).

1.3.3 ERBBs as oncogenic drivers

The ERBB family is well-known for its genetically altered members being linked to multiple human cancers. For instance, *EGFR* is frequently mutated in adenocarcinomas, in-frame exon 19 deletions and L858R point mutation being the most common mutations (Ochi et al., 2023). These mutations are suggested to result in constitutively active kinase by making the inactive conformation unstable (Yun et al., 2007). In contrast, *HER2* amplifications are common in breast, esophageal and gastric cancer (Arteaga & Engelman, 2014). In fact, 20 % of breast cancers present *HER2* amplifications, which are associated with poorer prognosis (Slamon et al., 1987). ERBB3 elicits its oncogenicity primarily by facilitating signaling through HER2 and EGFR but potentially oncogenic mutations in the *ERBB3* gene do exist as well (Arteaga & Engelman, 2014).

Targeted cancer therapies against EGFR and HER2, including small-molecule kinase inhibitors and monoclonal antibodies, exist in the clinic. EGFR-targeting drugs include, for example, third generation kinase inhibitor osimertinib and monoclonal antibody cetuximab, which are used for treating pancreatic, lung, colorectal as well as head and neck cancers (Chong & Jänne, 2013; Passaro et al., 2021). Examples of HER2-targeted drugs that are used for treating *HER2*-positive breast cancer include monoclonal antibody trastuzumab and kinase inhibitors lapatinib and neratinib, which also targets EGFR and ERBB4 (Loibl & Gianni, 2017).

Compared to the other members of the ERBB receptor family, the role of ERBB4 in cancer is more elusive. The results from many studies are contradictory part of the studies suggesting a tumor suppressor role (Suo et al., 2002; Thybusch-Bernhardt et al., 2001; Vidal et al., 2007), whereas other studies point towards an oncogenic role (Kim et al., 2016; Wege et al., 2018; Williams et al., 2015). This controversy could be explained by the complexity of ERBB4 signaling that has not been addressed in all studies: ERBB4 has multiple ligands and several isoforms that could activate different downstream signaling pathways and elicit different cellular responses (Segers et al., 2020).

Alternative splicing producing ERBB4 isoforms affects the extracellular juxtamembrane (eJM) region and the cytoplasmic (CYT) domain. Isoform JM-a contains 23 amino acids encoded by exon 16 and isoform JM-b, alternatively, contains 13 amino acids encoded by exon 15b. In addition, minor isoforms, including JM-c fully lacking the amino acids encoded by exon 16 and 15b, as well as JM-d containing the amino acids encoded by both exon 16 and 15b, have been reported. Furthermore, isoforms differing in the CYT domain include CYT-1 and CYT-2. CYT-

1 includes 16 amino acids encoded by exon 26, which are lacking in CYT-2 (Veikkolainen et al., 2011). These residues are required for PI3K binding making only CYT-1 able to bind PI3K (Elenius et al., 1999).

The exon 16 of *ERBB4* encodes a cleavage site for tumor necrosis factor-α converting enzyme (TACE), and, therefore, JM-a but not JM-b can be cleaved by this enzyme. The cleavage by TACE results in an extracellular fragment of 120 kDa in size and another 80 kDa fragment containing a couple extracellular residues, transmembrane domain, and cytoplasmic domain. The 80 kDa fragment can be further cleaved by γ-secretase releasing the intracellular domain ($s80^{HER4}$) (Muraoka-Cook et al., 2009; Ni et al., 2001).

The cleavable JM-a isoforms have been associated with oncogenic potential. For instance, multiparous mice develop mammary tumor lesions upon overexpression of JM-a CYT-1 isoform of *ERBB4* (Wali et al., 2014). Furthermore, JM-a CYT-1 and JM-a CYT-2 overexpression has been reported in human breast cancer and overexpressed JM-a CYT-2 has been shown to increase breast cancer cell proliferation *in vitro* (Määttä et al., 2006).

1.4 Resistance to targeted cancer therapies

1.4.1 Scope of the issue

Targeted anti-cancer therapies have become widely used cancer treatments over the past few decades. Although these therapies have been greatly beneficial for numerous patients, treatment resistance is an enormous issue. The majority of the patients develop drug resistance eventually despite good initial response (Shen et al., 2020). For instance, patients with *BRAF*-mutated melanoma, *EGFR*-mutated lung adenocarcinoma or lung adenocarcinoma with *ALK* rearrangements, who are treated with targeted therapies, relapse typically in 6 to 12 months (Obenauf et al., 2015).

1.4.2 Different types of kinase inhibitor resistance mechanisms

Development of resistance to kinase inhibitors is complex and can occur through various mechanisms including mutations in target genes, bypass signaling pathways as well as changes in tumor microenvironment, cell metabolism and inhibition of cell death. The mutations in drug target genes can make kinase inhibitors unable to bind their target kinase or, alternatively, result in conformational changes altering the target kinase activity (Yang et al., 2022). For example, *EGFR* T790M mutation confers resistance to EGFR-targeting inhibitors erlotinib and gefitinib by increasing the receptor's affinity to ATP. Therefore, erlotinib and gefitinib, which inhibit EGFR by binding competitively to the ATP-binding site, cannot elicit their function (Suda et al., 2009; Yun et al., 2007).

On the other hand, signaling molecules downstream from the drug target can mutate, becoming constantly active. Alternative receptors, which can activate the same downstream signaling pathways as the target kinase, can also become activated. In these ways the signaling through the targeted kinase can be bypassed (Yang et al., 2022).

1.4.3 Primary and acquired resistance

Cancer drug resistance can be divided into primary and acquired resistance. Primary resistance refers to resistance present upon the start of the initial treatment meaning that treatment does not lead to tumor shrinkage. Acquired resistance, on the other hand, develops over time after complete initial response, which is defined as lack of detectable evidence of cancer. Primary resistance is further divided into intrinsic and adaptive resistance. Intrinsic resistance refers to a pre-existing genetic alteration in the cancer cells that confers resistance to the therapy. In contrast, cancer cells with adaptive resistance can rapidly change their oncogenic signaling avoiding cell death upon start of the initial treatment (Cabanos & Hata, 2021).

Acquired resistance, in contrast, can develop in two ways. First, resistant cancer cell clones, which exist in the tumor in low frequency, can expand due to the selective pressure created by the drug treatment. Second, resistance can develop through so called drug-tolerant persister cells (Cabanos & Hata, 2021). Interestingly, it has been demonstrated that NSCLCs can become therapy resistant through *EGFR* T790M mutation either by selection of pre-resistant clones carrying *EGFR* T790M mutation or by mutation in drug-tolerant persister cells (Hata et al., 2016). Drug-tolerant persister cells are defined as slowly cycling or quiescent cancer cells that survive the drug therapy without acquiring mutations that cause therapy resistance (Cabanos & Hata, 2021). In clinical context the drug-tolerant persister cells can be also called residual disease, which refers to the cells that remain after maximum response to the treatment (Boumahdi & de Sauvage, 2020).

The tolerant state of the cancer cells is likely caused by epigenetic or nongenetic mechanisms. The state is suggested to be reversible meaning that the cells can regain drug sensitivity and start to proliferate once the treatment is discontinued (Cabanos & Hata, 2021; Marine et al., 2020; Shen et al., 2020). Interestingly, Sharma et. al. detected a subpopulation of cancer cells in *EGFR*-mutant NSCLC cell line that presents a reversible drug-tolerant state with G1 arrest upon treatment with 100-fold higher erlotinib concentrations than the IC50 value. Upon withdrawal of the drug the cells started proliferating and regained the sensitivity to EGFR-targeting kinase inhibitors within nine doublings (Sharma et al., 2010). Nevertheless, if the drug treatment is continued for an extended time period, the drug-tolerant persister cells can acquire mutations that make them fully resistant to the therapy. The resulting therapy-resistant cancer cells can start proliferating despite the drug exposure and cause disease relapse (Cabanos & Hata, 2021; Marine et al., 2020; Shen et al., 2020).

The emergence of the drug-tolerant persister cells could be explained by two models, namely Lamarckian induction, and Darwinian selection. According to Lamarckian induction, drug persistence is treatment-induced and not pre-existing. In other words, the drug-containing environment directs the cancer cells towards a more favorable phenotype by change in gene expression profile (Marine et al., 2020; Shen et al., 2020). In contrast, according to Darwinian selection, a subpopulation of cancer cells would present pre-existing tolerance to the therapy based on their transcriptional profile and once the drug is introduced the proportion of these cells increases. Nevertheless, Lamarckian induction and Darwinian selection are not exclusive and likely both contribute to the emergence of the drug-tolerant persister cells (Boumahdi & de Sauvage, 2020). It has been shown that the expression levels of genes that promote therapy resistance vary on single-cell level in untreated cancer cells. Shaffer et. al. demonstrated how subpopulation of *BRAF* V600E -mutated melanoma cells that express high levels of resistance markers before being exposed to BRAF inhibitor vemurafenib undergo epigenetic programming once being exposed to the drug. This epigenetic programming shifts the pre-tolerant melanoma cells into a more stable vemurafenib-tolerant state (Shaffer et al., 2017).

1.4.4 NRG1/ERBB axis in drug resistance

Growth factors, including NRG1, have been linked to resistance development towards targeted therapies in many cancer contexts. Exogenous NRG1 has been shown to elicit strong resistance to lapatinib in *HER2*-amplified breast cancer cell lines. It also confers resistance to crizotinib in *MET*-amplified cancer cell lines and to fibroblast growth factor receptor inhibitors in *fibroblast growth factor receptor*-amplified cancer cell lines. Complete or partial resistance was also seen in some *BRAF* V600E melanoma cell lines treated with a BRAF inhibitor (Wilson et al., 2012).

In another study by Cheng et. al. NRG1 has been demonstrated to confer resistance to MEK inhibition in metastatic uveal melanoma cell lines (Cheng et al., 2015). NRG1 also drives resistance to trastuzumab in *HER2*-amplified breast cancer cells and this effect seems to be mediated by activation of ERBB3 receptors (Yang et al., 2017). Moreover, if the action of NRG1 is blocked by antibodies, response to conventional chemotherapy is improved *in vivo* (Hegde et al., 2013).

Previous results from our group also demonstrate how exogenous NRG1 drives resistance to targeted therapies in several oncogene-addicted cancer cell lines. Additionally, when cells are treated with standard-of-care (SOC) targeted therapy treatments, NRGs and their receptors are upregulated in multiple oncogene-addicted cancer cell lines including *BRAF* V600E -mutant melanoma and colorectal cancer, *HER2*-amplified breast cancer as well as in NSCLC cell lines harboring either *ALK* fusion, *MET* amplification or *EGFR* exon 19 deletion (Takala, 2022). This suggests that the cancer cells may use signaling through NRG/ERBB axis as an adaptation mechanism in order to survive under drug exposure.

1.5 CRISPR-Cas9 as a tool for gene knockout studies

CRISPR-Cas9 is a tool for gene editing and can be used to create desired gene knockouts to study necessity of a certain gene to a biological process of interest. The tool has been developed from an adaptive immune system of bacteria against viruses. This immune system allows bacteria to recognize genetic material from viruses that they have been infected by previously and destroy the viral DNA by cleaving it into fragments (Wang et al., 2022).

The CRISPR-Cas9 system used for gene editing relies on a gRNA and Cas9 nuclease. The gRNA directs the nuclease precisely to the correct location on the cellular genome, where the Cas9 nuclease creates a double-strand break. An important aspect to note when designing CRISPR experiments with the most used Cas9, SpCas9, is that the DNA sequence to be cleaved must have a 3-bp-long sequence motif, NGG, which is referred to as PAM sequence. The PAM sequence is required for triggering the activity of Cas9 (Wang et al., 2022).

In the immune system of bacteria, the gRNA is formed by two RNA molecules, tracrRNA containing the constant region required for binding of Cas9 nuclease, and crRNA containing the variable region, which guides the Cas9 nuclease to the correct genomic region. For genome editing purposes, it is possible to use either the tracrRNA and crRNA duplex or single guide

RNA, where the crRNA and tracrRNA are produced as a single RNA molecule (Turk & Spencer, 2019).

The gRNA and Cas9 nuclease can be delivered into the cells as gRNA and Cas9 nuclease -encoding DNA incorporated into single or several plasmid(s), mRNA or as RNP, which contains the Cas9 nuclease in a complex with the gRNA (Horodecka & Düchler, 2021). Of these delivery options RNPs have been shown to be the most effective and less cytotoxic *in vitro* (Kouranova et al., 2016; Lattanzi et al., 2019). Several strategies for delivering RNPs into cells exist and include lipid reagents as well as electroporation, where permeability of the cell membrane is increased using electrical field pulses (Horodecka & Düchler, 2021). Nucleofection is one electroporation-based method, which utilizes electric pulse and optimized buffers for delivery. It is claimed to be superior in efficacy and low cytotoxicity over traditionally used methods for electroporation (Đorđević et al., 2022).

Once the double-strand break in the DNA has been introduced by the Cas9 nuclease, the cells have two approaches for repairing it, one of which is nonhomologous end joining. This method is prone to errors and, therefore, often leads to removal or addition of bases resulting in in-frame indels or frameshift mutations. Frameshift mutations lead to premature stop codons and thus cause loss of functional protein due to truncation, producing a knockout (Wang et al., 2022).

1.6 Aims and hypotheses

Based on the previous results in the group, NRGs and their receptors are upregulated in oncogene-addicted cancer cell lines upon SOC targeted therapy (Takala, 2022). Hence, the main goal of this thesis was to determine functional relevance of this upregulation in drug-tolerant persister cells.

1.6.1 Aims

The thesis work was divided into two aims. The first aim was to examine the ERBB receptor and downstream signaling activation in drug-tolerant persister cells to investigate if the increased expression of NRGs and their ligands induce activation of ERBB receptors and downstream signaling. The second aim was to examine the necessity of NRG/ERBB signaling for the survival of the drug-tolerant persister cells.

1.6.2 Hypotheses

As the previous results in the group demonstrate that targeted therapy is associated with the upregulation of the NRG/ERBB axis in oncogene-addicted cell lines, we hypothesized that the ERBB receptor activation and downstream signaling is increased upon treatment by targeted therapies in oncogene-addicted cancer cell lines. Furthermore, we hypothesized that NRG/ERBB signaling is crucial for driving drug tolerance in oncogene-addicted cancers.

2 Results

2.1 Activation of ERBB signaling in oncogene-addicted cancer cell lines upon SOC targeted treatment

2.1.1 Robust reactivation of ERBB signaling upon 10-day SOC targeted treatment in H3122 and HT-29 cells

To evaluate the activation of ERBB receptors and downstream signaling upon SOC targeted therapy treatment, six oncogene-addicted cancer cell lines were treated with SOC targeted therapies for 10 days. The included cell lines were A375 (*BRAF* V600E -mutated melanoma), BT-474 (*HER2*-amplified breast cancer), EBC-1 (*MET*-amplified NSCLC), H3122 (*ALK*-rearranged NSCLC), HCC827 (*EGFR* exon 19 -deleted NSCLC) and HT-29 (*BRAF* V600E -mutated colorectal cancer). Activation of ERBB signaling as well as the total levels of the signaling proteins were analyzed by western blotting on three timepoints including untreated cells and cells treated for 1 and 10 days. The level of phosphorylated signaling protein was considered to correspond to the level of activated protein.

Compared to the untreated control, the amount of phosphorylated ERK diminished on the first day of drug treatment in crizotinib-treated H3122, osimertinib-treated HCC827 cells and A375 cells treated with dabrafenib and trametinib (**Figure 2D, 2E** and **2A**). In these cells ERK activation markedly increased on day 10 in relation to day 1, reaching a higher level compared to the untreated control in A375 and H3122 cells. Elevated activation of ERK on day 10 relative to untreated control and cells treated for 1 day could also be observed in HT-29 cells treated with a combination of dabrafenib and cetuximab (**Figure 2F**).

Furthermore, AKT activation exhibited a similar pattern to ERK activation. In H3122 and HT-29 cells, the activation was elevated on day 10 in comparison to control after initial reduction on day 1 (**Figure 2D** and **2F**). HCC827 cells showed a similar pattern in AKT activation but the reactivation on day 10 did not exceed the level of activation in the untreated control (**Figure 2E**). Like other cell lines, lapatinib-treated BT-474 showed a marked reduction of phosphorylated AKT and ERK on day 1 of treatment relative to untreated control (**Figure 2B**). The level of activation of both downstream signaling proteins was slightly elevated on day 10 compared to day 1 but the difference was not as pronounced as in other cell lines.

In A375 cells, the total ERBB2 and ERBB3 levels were elevated upon the treatment relative to untreated control (**Figure 2A**). However, this cell line demonstrated very minimal levels of ERBB receptor activation. Detection of phosphorylated or total ERBB4 proved unsuccessful across cell lines, likely due to low basal expression of the receptor.

Decreased ERBB2 activation in lapatinib-treated BT-474 confirmed the effectiveness of the drug in this cell line (**Figure 2B**). Activation of EGFR and ERBB3 was also dampened in the drug-treated cells. The total EGFR and ERBB2 levels remained similar in all timepoints whereas a very slight increase in overall ERBB3 level can be observed on days 1 and 10 compared to the untreated control.

Due to high sensitivity to crizotinib treatment, obtaining a proper sample for western blotting from crizotinib-treated EBC-1 cells remained problematic (**Figure 2C**). First, the cells were treated with a concentration of 1 μM but also an experiment with a lowered concentration was carried out. The lowered concentration was chosen to be 100 nM, which is the lowest concentration that still produces the maximum response to the drug according to dose-response experiments previously performed in the group. Even with the lower drug concentration or by pooling several technical replicates together upon sample preparation, obtaining a proper western blot sample was not successful and no further experiments were conducted using EBC-1 cells.

Although clear reactivation of AKT and ERK was observed in osimertinib-treated HCC827 cell line on day 10 of treatment, it did not correlate with activation of the ERBB receptors (**Figure 2E**). Dampened activation of EGFR in the drug-treated cells confirmed that the osimertinib treatment was effective in this cell line. Activated ERBB2 or ERBB3 were not detected in the treated samples. Nevertheless, an increasing trend in the total ERBB2 level was observed upon treatment. In addition, the overall ERBB3 level spiked on day 1 compared to the other timepoints.

In H3122 cells, EGFR, ERBB2 and ERBB3 activation as well as total ERBB2 and ERBB3 levels were increased on day 10 when contrasted with untreated control and cells treated for 1 day (**Figure 2D**). In HT-29 cells, the same phenomenon was observed in EGFR and ERBB2 activation as well as in overall ERBB2 level (**Figure 2F**). In the same cell line, the total EGFR level decreased on day 1 compared to the untreated control followed by an increase on day 10 relative to day 1.

In conclusion, the RAS/RAF/MEK/ERK downstream signaling pathway was strongly reactivated on day 10 in four out of six investigated cancer cell lines after initial downregulation on day 1. The PI3K/AKT pathway was also notably reactivated on day 10 in half of the cell lines. In H3122 and HT-29 cells the reactivation of these downstream signaling pathways correlated with activation of EGFR, ERBB2 and ERBB3 or EGFR and ERBB2, respectively.

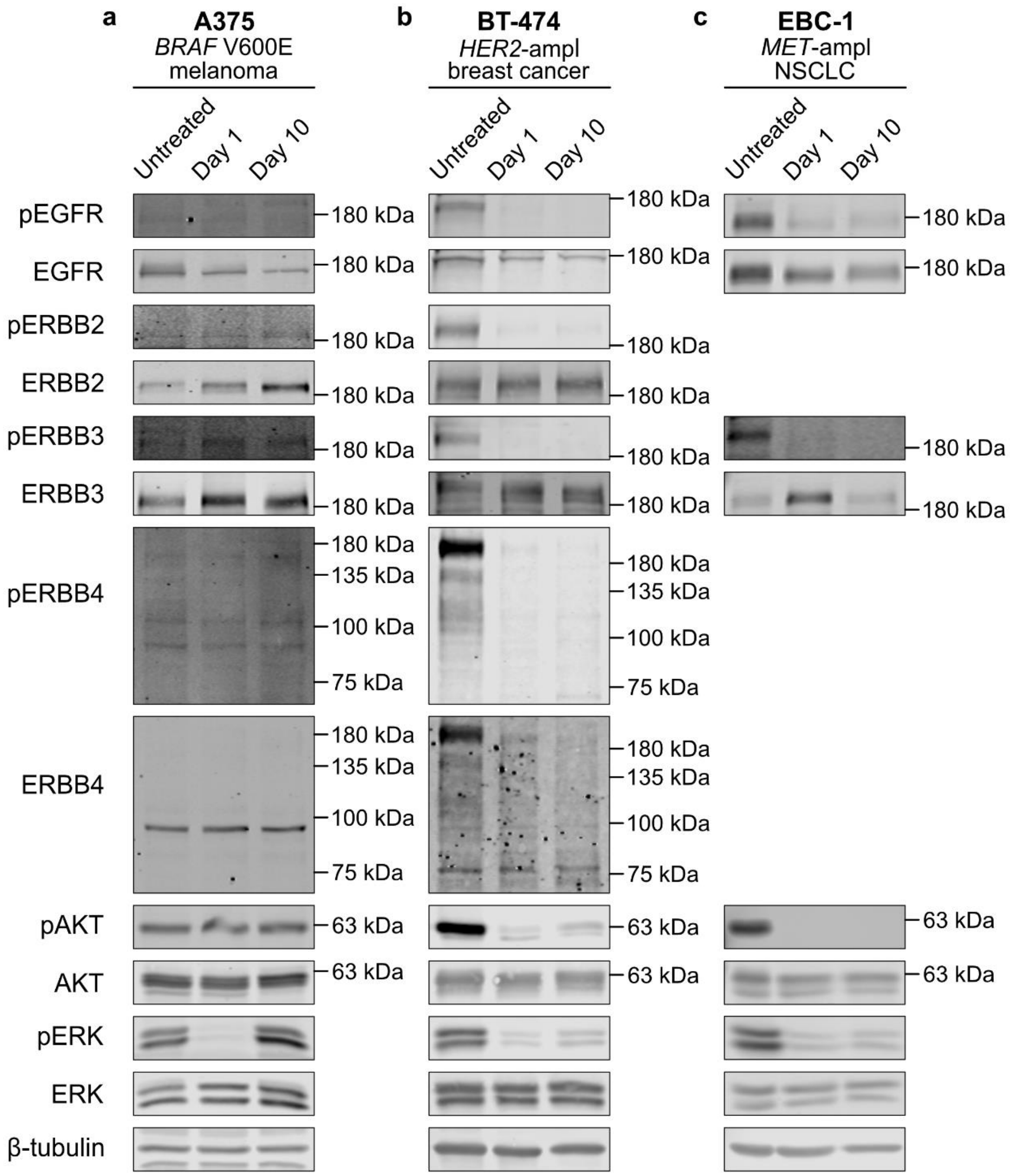

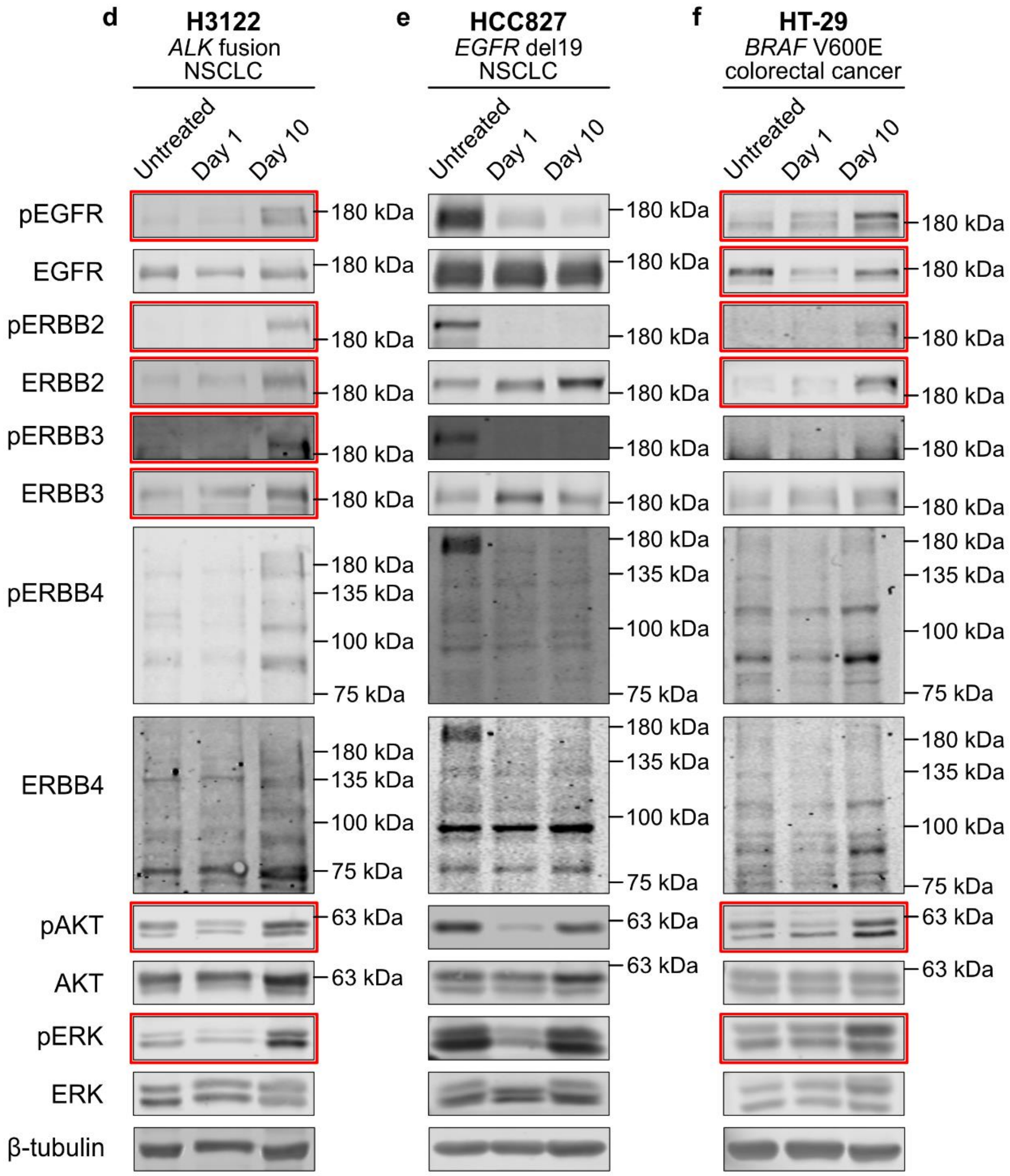

Figure 2. ERBB signaling was reactivated upon 10-day treatment with SOC targeted therapy in multiple oncogene-addicted cell lines. Six oncogene-addicted cell lines were treated with SOC targeted therapies (**a**, A375: 1 µM dabrafenib + 100 nM trametinib, **b**, BT-474: 1 µM lapatinib, **c**, EBC-1: 1 µM crizotinib, **d**, H3122: 1 µM crizotinib, **e**, HCC827: 1 µM osimertinib and **f**, HT-29: 1 µM dabrafenib + 10 µg/ml cetuximab) for 10 days and western blotting was used to analyze ERBB signaling activation. β-tubulin was used as a loading control. Out of three independent experiments the results from the most representative are shown here. The expected ERBB receptor sizes are 175 kDa for EGFR, 185 kDa for ERBB2 and ERBB3, 180 kDa for ERBB4 and 80 kDa for s80^{HER4}.

2.1.2 ERBB receptor reactivation upon SOC targeted treatment peaks at 10 to 20 days in H3122 and HT-29 cells

Five oncogene-addicted cancer cell lines A375, BT-474, H3122, HCC827 and HT-29 were treated with SOC targeted therapies for 30 days to address if ERBB signaling activation changed during the evolution of the drug-tolerant cell population. The activation and total signaling protein levels were again analyzed by western blotting, with samples collected on days 1, 10, 20 and 30 after beginning the drug treatment as well as from untreated control cells. The level of phosphorylated signaling protein was considered equal to the level of activated protein.

In all cell lines the ERK activation was decreased on day 1 in comparison to the untreated control cells and elevated on days 10 to 30 relative to day 1 (**Figure 3**). The ERK activation reached its peak on days 10 and 30 in A375 cells treated with dabrafenib and trametinib, on day 10 in HT-29 cells treated with dabrafenib and cetuximab and on day 20 in lapatinib-treated BT-474 cells (**Figure 3A, 3E** and **3B**). Again, the AKT activation levels followed the same pattern as ERK activation in all investigated cell lines excluding BT-474. The most notable difference in AKT activation between days 1 and 10-30 was observed in crizotinib-treated H3122 cells and HT-29 cells (**Figure 3C** and **3E**). In H3122, AKT activation peaked on day 20, whereas in HT-29 the level of activation remained similar on days 10 and 20, diminishing slightly on day 30.

Total ERBB2 level in A375 cells was increased in day 10 and 20 samples in relation to untreated control and day 1 samples (**Figure 3A**). However, activation of all ERBB receptors was low in this cell line. Furthermore, as the overall protein amount in the A375 30-day sample was low, phosphorylated, and total EGFR and ERBB2 were not able to be blotted.

In lapatinib-treated BT-474 and osimertinib-treated HCC827 cells, ERBB2 and EGFR activation, respectively, were diminished indicating proper inhibition by the drugs (**Figure 3B** and **3D**). BT-474 cells showed slightly elevated total ERBB3 level on day 1 of the treatment compared to the untreated control. From day 10 the ERBB3 level began to decrease. The levels of EGFR and ERBB2 were also decreasing in BT-474 cells during the course of the treatment. In contrast, in HCC827 cells the total ERBB2 level was elevated on days 1 to 20 in relation to the untreated control, being the highest on days 10 and 20. However, the activation of ERBB2 on days 1 to 20 was lower relative to the control. On day 30, the ERBB2 activation was increased compared to days 1 to 20 but still lower in comparison to the control. Interestingly, the total ERBB3 level in HCC827 peaked on day 1.

In H3122 cells the activation of EGFR, ERBB2 and ERBB3 increased on days 10 to 20 in comparison to control and day 1 samples, and notable reduction was observed on day 30 (**Figure 3C**). In HT-29 cells the same phenomenon was notably visible in ERBB2 activation (**Figure 3E**). EGFR activation, in turn, reached its peak on day 10 in HT-29 cells. The total EGFR levels correlated well with the phosphorylated receptor level in both H3122 and HT-29. ERBB2 activation, in turn, peaked on day 20 in H3122 and on day 10 in HT-29 with overall ERBB2 level strongly correlating with the phosphorylated receptor level. In HT-29 cells the total ERBB3 level was elevated on days 1 to 20 relative to the remaining samples. Again, detection of phosphorylated and total ERBB4 levels in all cell lines was overall unsuccessful. However, in H3122 cell line total ERBB4 level seemed to be increased on days 10 and 20 compared to other timepoints and untreated control.

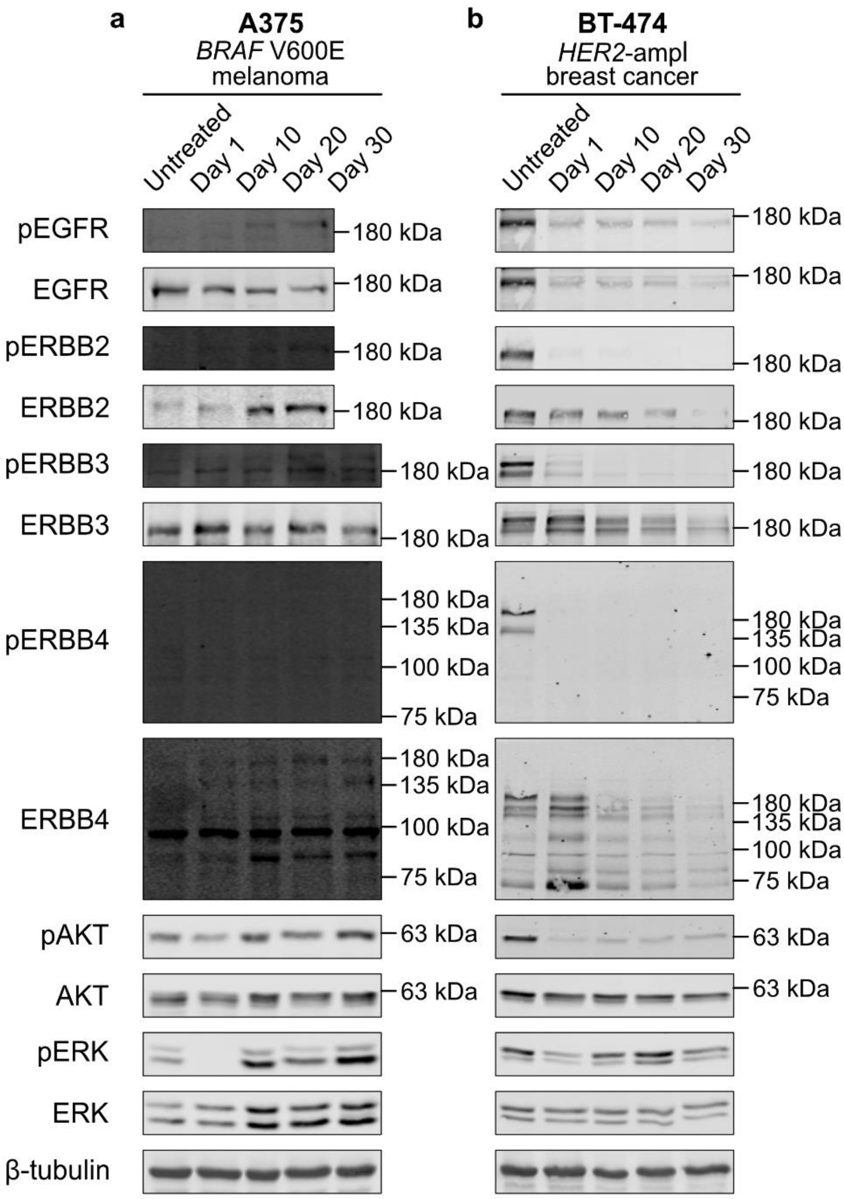
a
A375
BRAF V600E
melanoma
b
BT-474
HER2-ampl
breast cancer
Untreated
Day 1
Day 10
Day 20
Day 30
pEGFR
EGFR
pERBB2
ERBB2
pERBB3
ERBB3
pERBB4
ERBB4
pAKT
AKT
pERK
ERK
β-tubulin
180 kDa
135 kDa
100 kDa
75 kDa
63 kDa

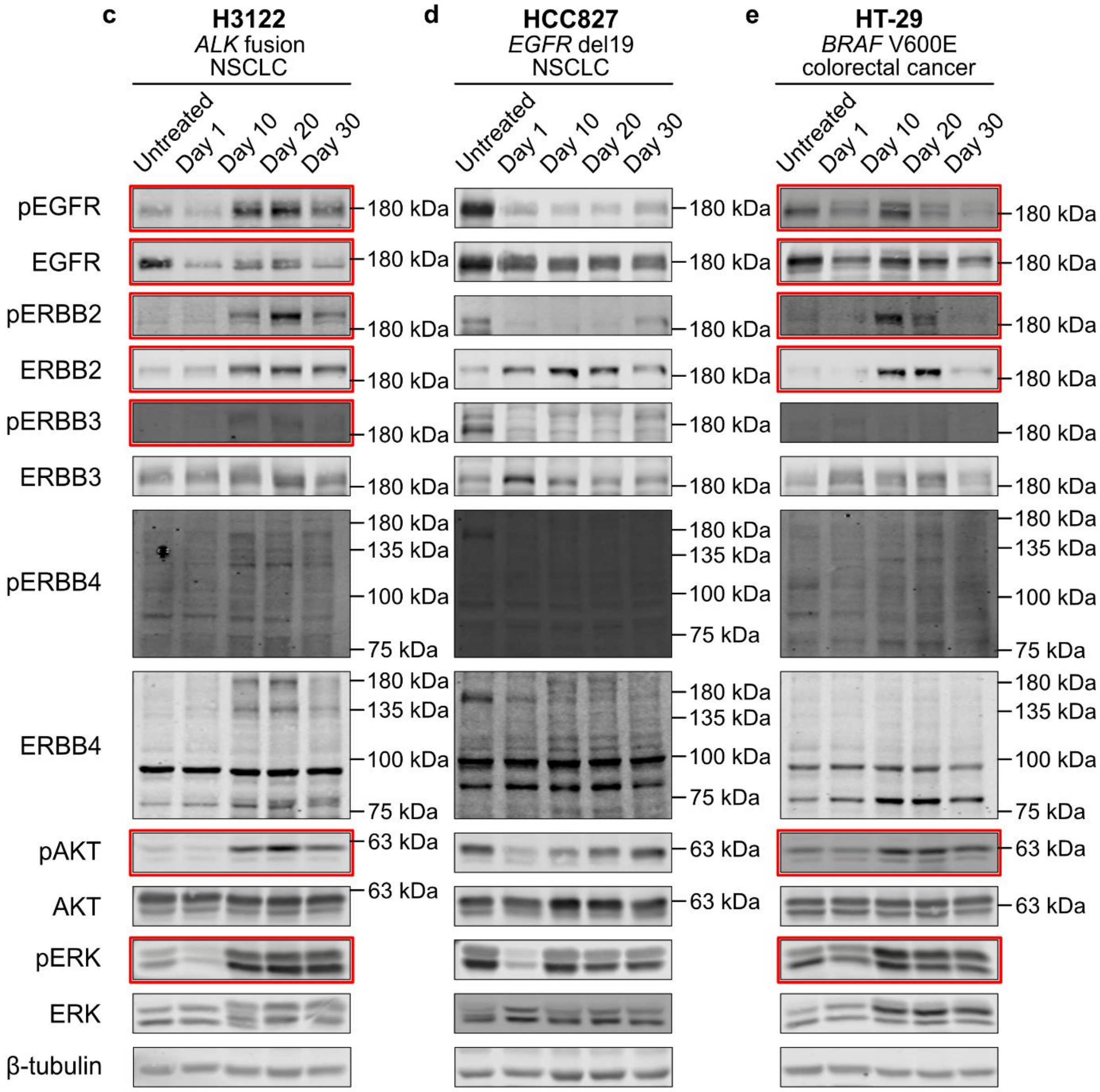

Figure 3. ERBB receptor reactivation upon SOC targeted therapy treatment peaked around 10 to 20 days in H3122 and HT-29 cells. Five oncogene-addicted cell lines were treated with SOC targeted therapies (**a**, A375: 1 µM dabrafenib + 100 nM trametinib, **b**, BT-474: 1 µM lapatinib, **c**, H3122: 1 µM crizotinib, **d**, HCC827: 1 µM osimertinib and **e**, HT-29: 1 µM dabrafenib + 10 µg/ml cetuximab) for 30 days and western blotting was used to study ERBB signaling activation. β-tubulin was used as a loading control. The results are from a single experiment. The expected ERBB receptor sizes are 175 kDa for EGFR, 185 kDa for ERBB2 and ERBB3, 180 kDa for ERBB4 and 80 kDa for $s80^{HER4}$.

Additionally, growth curves depicting change in cell number over the course of the 30-day drug treatment were produced to detect the timepoint, where the cells started proliferating again, which would indicate resistance development. A375 and BT-474 cells were highly sensitive to the targeted drugs. The number of A375 and BT-474 cells decreased the whole duration of the 30-day drug treatment the cell number being 90 % lower on day 30 compared to the time of seeding (**Figure 4A** and **4B**). The trend in H3122 cell number was increasing from day 1 onwards reaching 262 % increase on day 30 in comparison to the number of cells originally seeded on the cell culturing dish (**Figure 4C**). The number of HCC827 cells decreased from day 1 until day 20 but due to the high standard deviation, it is hard to conclude the trend on day 30 (**Figure 4D**). The number of HT-29 cells decreased from day 1 to day 10 and thereafter the number of cells started to increase reaching 95 % more cells on day 30 relative to the time of seeding the cells (**Figure 4E**). In conclusion, A375 and BT-474 were the most sensitive cell lines to the used targeted therapies, whereas H3122 seemed to be the least sensitive cell line followed by HT-29.

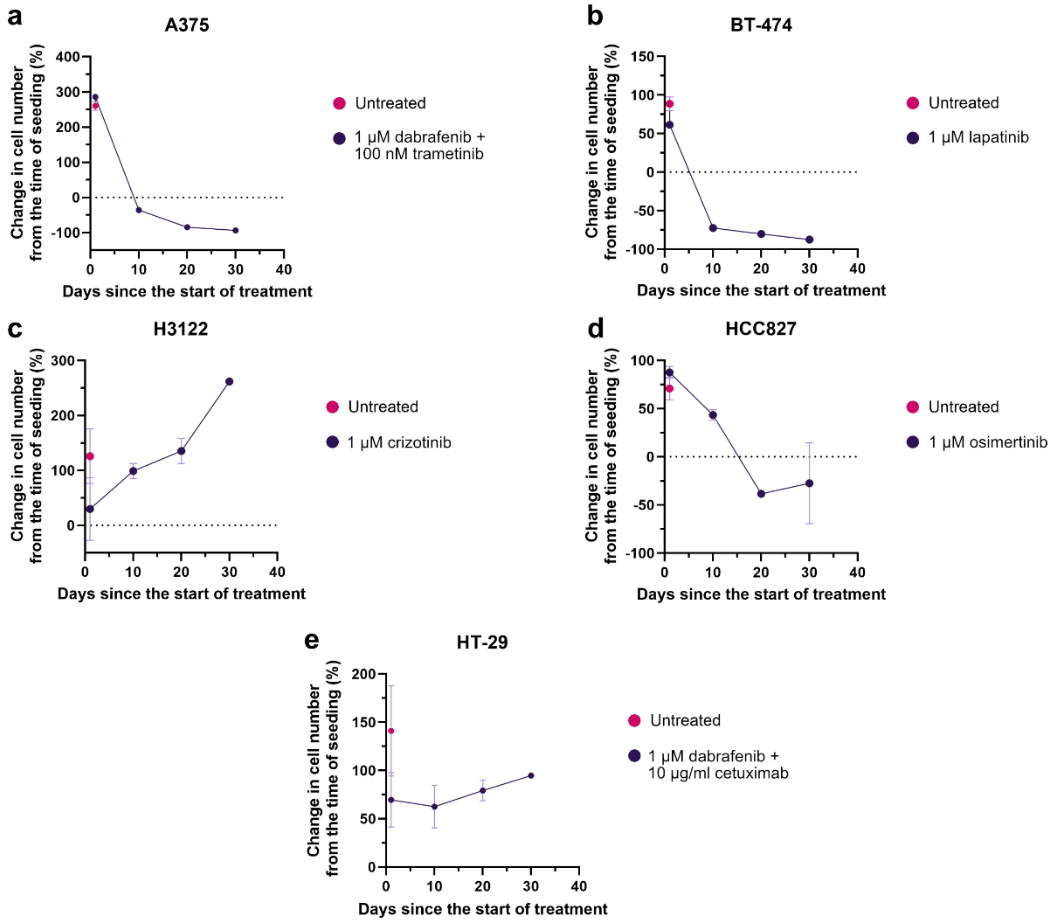

Figure 4. Change in cell number upon 30-day SOC targeted therapy treatment. Five oncogene-addicted cell lines were treated with SOC targeted therapies for a total of 30 days. The number of cells was counted at 1, 10, 20 and 30 days after beginning the treatment. Change in the cell number compared to the number of cells seeded on the plate before start of the treatment (0 %) is presented. The data is shown as a mean from two technical replicates and the error bars represent standard deviation.

Overall, the ERBB signaling activation on days 1 and 10 closely resembled the results obtained from the previously described similar 10-day experiments (section 2.1.1). In general, the total and phosphorylated protein levels correlated, indicating that elevated protein levels corresponded to increased protein activation. This correlation was the weakest in HCC827 cell line. The peak in ERBB signaling activation was observed in most cell lines on 10 to 20 days of the drug treatment. H3122 and HT-29 cells, the least therapy-sensitive cell lines characterized by the highest increase in cell number over the 30-day treatment period, also displayed the most robust reactivation of the ERBB signaling axis.

2.2 Necessity of NRG/ERBB signaling for survival of drug-tolerant cells

The necessity of signaling through ERBB receptors for the survival of drug-tolerant cells was assessed in H3122 and HT-29 cells, which exhibited the most vigorous activation of the ERBB signaling axis upon SOC targeted therapy treatment. This was achieved by knocking out the ERBB receptors individually using CRISPR-Cas9 and treating the resulting knockout cell pools consisting of homozygous and heterozygous knockout cells, wild-type cells as well as cells with in-frame indels with the same SOC targeted therapies as previously.

2.2.1 Selection of best gRNAs for knocking out *ERBBs* using CRISPR-Cas9

The efficacy of gRNAs for knocking out ERBB receptors by CRISPR-Cas9 was assessed in T47D cells, which were chosen for the purpose as they express all ERBB receptors. CRISPR-Cas9 system was delivered into the cells as RNP using nucleofection and the level of the ERBB receptors in the CRISPR-treated cells 3 days post-nucleofection was analyzed by western blot. Two gRNAs per *ERBB* gene were tested.

Nucleofection efficiency was evaluated by nucleofecting pmaxGFP^{TM} plasmid, which encodes GFP, into T47D cells. The cells were imaged 24 h after nucleofection. Fluorescence and bright-field images were captured from three parts of the cell culturing dish. Total cell area from the bright-field images and the area of the cells expressing GFP from the fluorescence images were determined using ImageJ software. Nucleofection efficiency was determined as total area of GFP-expressing cells divided by the total cell area and the mean efficiency and standard deviation were calculated from the three image pairs. The nucleofection efficiency obtained in this way was 19.3 % (SD 6.4) (**Figure 5A**).

The gRNAs used to knock out *EGFR*, namely EGFR_AA and EGFR_AC, notably reduced overall EGFR abundance when contrasted with wild-type control (**Figure 5B**). The gRNA ERBB2_AB employed for *ERBB2* knockout, in turn, diminished the overall ERBB2 level slightly in relation to the wild-type control. However, the gRNAs employed for *ERBB3* or *ERBB4* knockouts did not result in reduction of the total ERBB3 or ERBB4 level, respectively.

Due to the limitations in time, additional gRNAs were not evaluated and the most efficient among those assessed were selected. Therefore, gRNAs EGFR_AA, ERBB2_AB, ERBB3_AA and ERBB4_AA were chosen to be used in the main experiments.

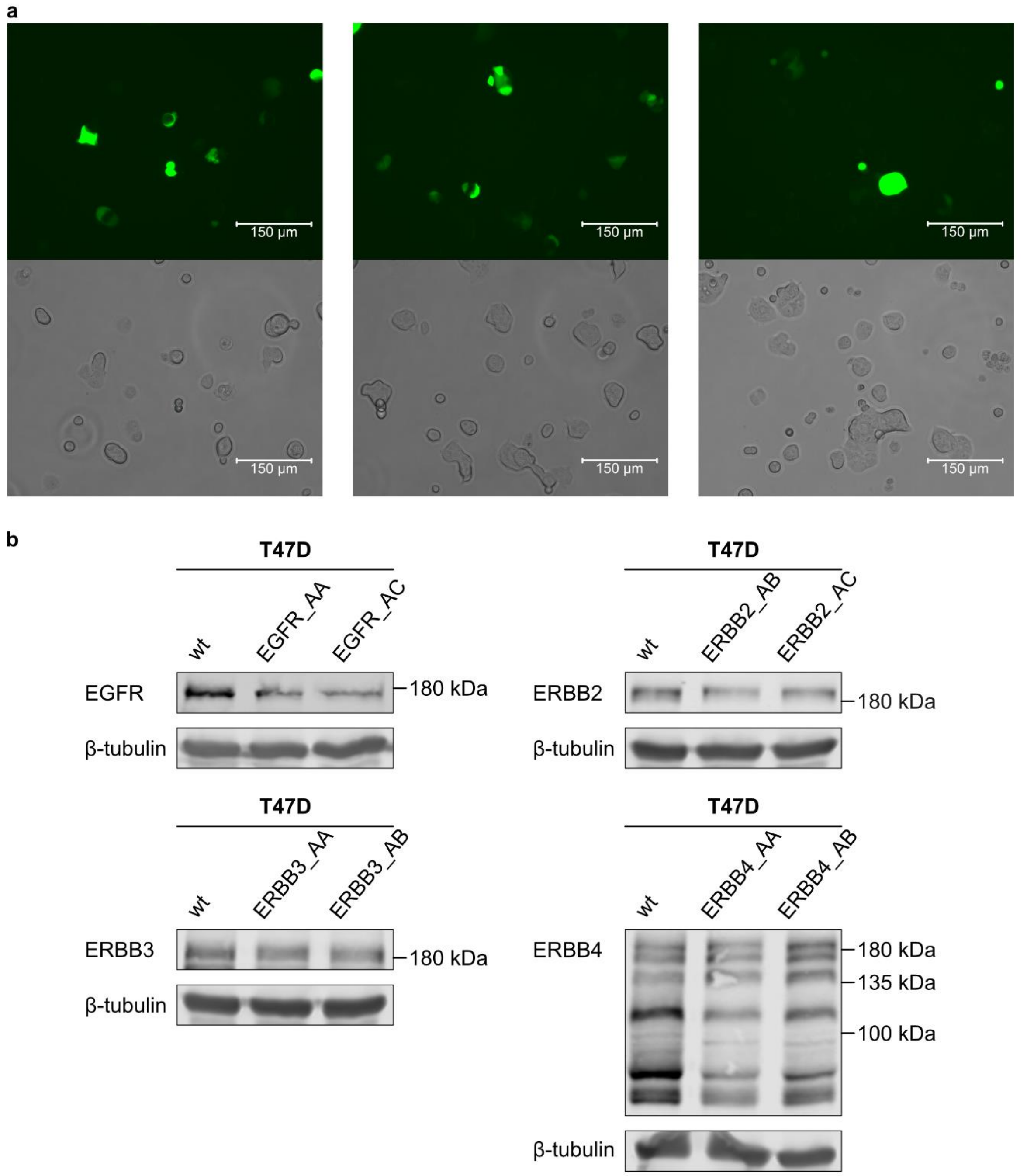

Figure 5. Nucleofection and CRISPR-Cas9 knockout efficiency in T47D cells. **a**, pmaxGFP™ plasmid was nucleofected into T47D cells to determine the nucleofection efficiency. The cells were imaged 24 h post-nucleofection. Fluorescence and bright-field images from three separate parts of the cell culturing dish were taken. The nucleofection efficiency was calculated as mean from the three image pairs and was defined as total area of GFP-positive cells/total cell area. The nucleofection efficiency determined in this way was 19.3 % (SD 6.4). Scale bars, 150 µm. **b**, gRNAs for knocking out ERBB receptors (2 per *ERBB* gene) were tested in T47D cells. CRISPR-Cas9 system was delivered into the cells as RNP using nucleofection. Knockout efficiency was analyzed by western blotting 3 days post-nucleofection. β-tubulin was used as a loading control. The expected ERBB receptor sizes are 175 kDa for EGFR, 185 kDa for ERBB2 and ERBB3, 180 kDa for ERBB4 and 80 kDa for s80^{HER4}. wt = wild-type.

2.2.2 CRISPR efficiency in H3122 and HT-29 cells

The efficiency of knocking out ERBB receptors in H3122 and HT-29 cells by CRISPR-Cas9 was evaluated by western blotting 7 days after introducing the CRISPR-Cas9 system into the cells by nucleofection. *EGFR* and *ERBB2* were sufficiently knocked out in H3122 cells as the total EGFR and ERBB2 levels were reduced in relation to the wild-type control as well as the other knockout cell pools (**Figure 6**). However, the efficiency of knocking out *ERBB3* remained poor. ERBB4 was not detected in any sample, likely due to the low basal expression of the receptor in both cell lines.

Unexpectedly, EGFR, ERBB2 and ERBB3 abundance in wild-type HT-29 sample were markedly higher compared to all *ERBB* knockout cell pools. The wild-type sample band exhibited greater compression in comparison to the remaining bands, thereby precluding accurate interpretation of the results. A repeat of the immunoblotting should be performed to enable reliable interpretation.

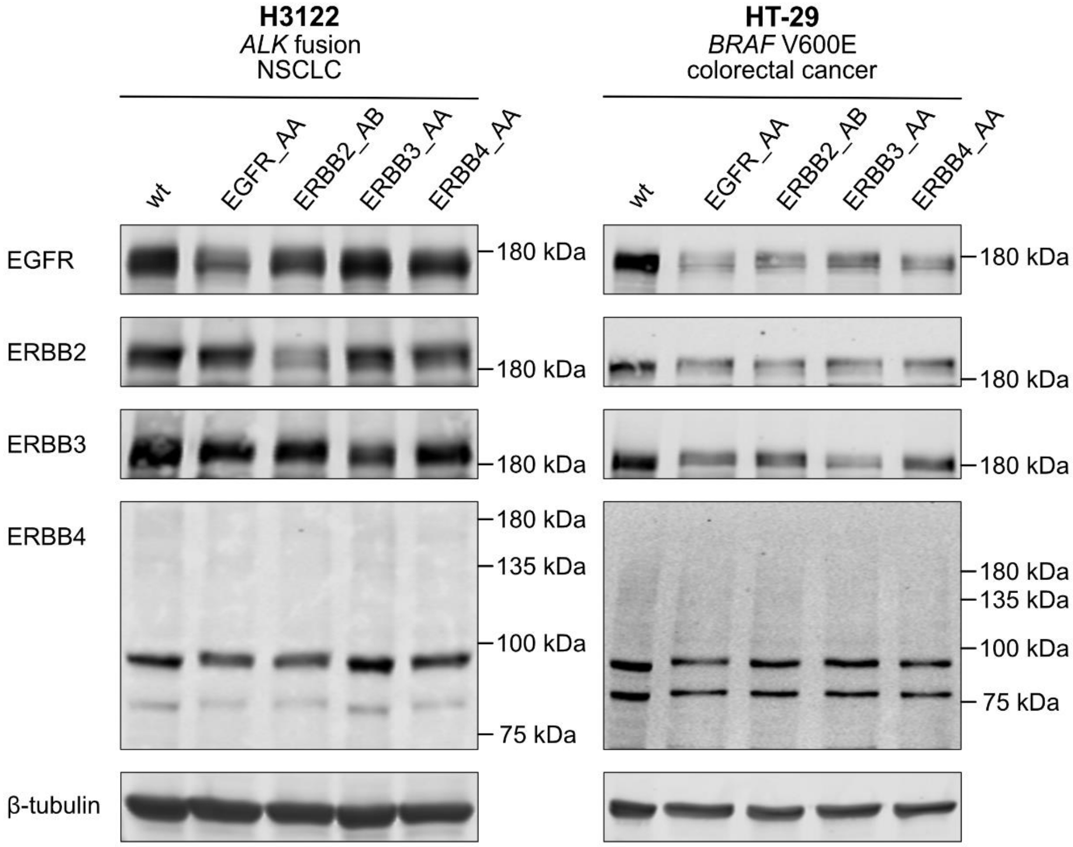

Figure 6. Western blotting analysis of CRISPR-Cas9 knockout efficiency in H3122 and HT-29 cells. ERBB receptors in H3122 and HT-29 cells were knocked out separately using CRISPR-Cas9. The cells were grown for 7 days before determining the knockout efficiency using western blotting. β-tubulin was used as a loading control. The expected ERBB receptor sizes are 175 kDa for EGFR, 185 kDa for ERBB2 and ERBB3, 180 kDa for ERBB4 and 80 kDa for s80^{HER4}. wt = wild-type.

2.2.3 Dependency of H3122 cells on EGFR, ERBB2, and ERBB3, and ERBB2 dependency in HT-29 cells

To study the necessity of the ERBB receptors for the survival of the drug-tolerant H3122 and HT-29 cells, ERBB receptors were knocked out separately in H3122 and HT-29 cells using CRISPR-Cas9, and the knockout cell pools, containing wild-type cells and cells with in-frame indels in addition to heterozygous and homozygous knockouts, were treated with SOC targeted therapies for 10 days. Genomic DNA from the drug-treated and untreated control cells was extracted and the genomic regions targeted by CRISPR-Cas9 were amplified by PCR. The correct PCR products of 207-229 bp in size were amplified successfully (**Figure 7A**). However, an additional band around 600-700 bp in size was detected when amplifying the CRISPR-targeted region in *ERBB3* gene. As a result, the correct PCR product had to be separated by agarose gel electrophoresis and purified from the gel.

The PCR products were sequenced by next-generation sequencing and the data processing was performed using CRISPResso2 software. CRISPR knockout efficiency, defined as the proportion of frameshift mutation allele reads in the untreated control sample, was overall low in all samples (**Figure 7B**). The proportion of alleles with a frameshift mutation was higher in H3122 cells compared to HT-29 cells, varying between 30 % and 56 %. In HT-29 cells, *ERBB3* was knocked out with the highest efficiency of 45 %, although the percentage of frameshift mutation alleles varied between 16 % and 22 % when knocking out *EGFR*, *ERBB2* or *ERBB4*.

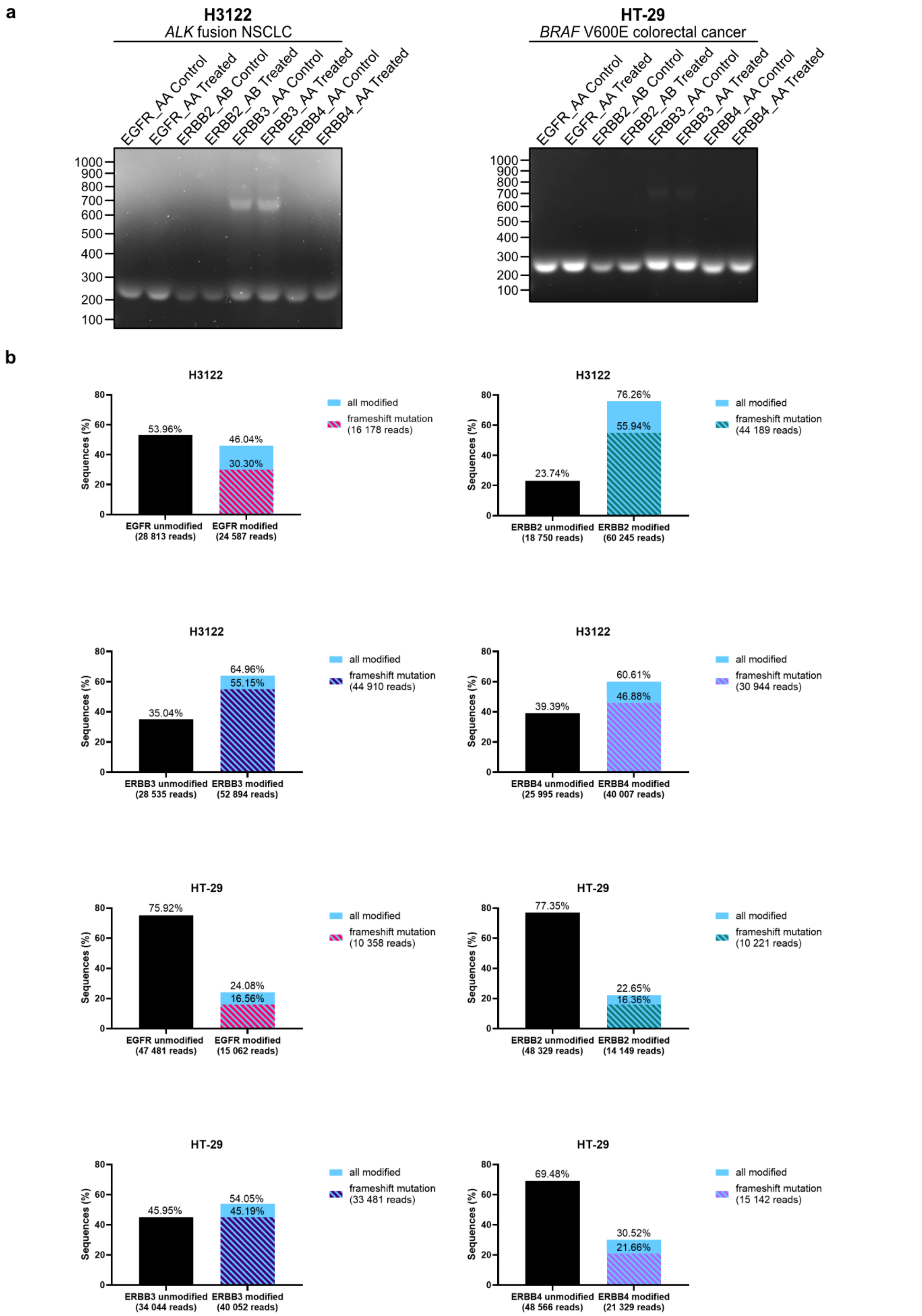

Figure 7. CRISPR knockout efficiency determined as the proportion of reads of alleles with frameshift mutation was overall low in H3122 and HT-29 cells. ERBB receptors were knocked out separately by CRISPR-Cas9 in H3122 and HT-29 cell lines and the cells were treated with targeted

therapies (H3122: 1 µM crizotinib and HT-29: 1 µM dabrafenib + 10 µg/ml cetuximab) for 10 days. Genomic DNA from the cells was extracted, the region targeted by CRISPR-Cas9 was amplified by PCR and the PCR products were sequenced by next-generation sequencing. **a**, Amplification of PCR products with the correct size was determined by agarose gel electrophoresis. PCR product sizes: EGFR_AA 228 bp, ERBB2_AB 207 bp, ERBB3_AA 229 bp and ERBB4_AA 212 bp. **b**, To depict CRISPR knockout efficiency, the percentage of reads with unmodified, modified and frameshift mutation alleles from untreated control samples were plotted.

The fold change to untreated cells (day 0) in variant allele frequency (VAF) was plotted for unmodified and frameshift mutation alleles against treatment time. During crizotinib treatment in H3122 cells, the proportion of alleles with a frameshift mutation declined while the proportion of wild-type allele increased, when either *EGFR*, *ERBB2* or *ERBB3* was knocked out (**Figure 8A**). The strongest effect was observed when either *EGFR* or *ERBB2* was knocked out. There, the frequency of frameshift mutation alleles decreased 0.7 and 0.8 fold as well as wild-type alleles increased 1.2 and 1.3 fold on day 10 of treatment compared to day 0, respectively. In HT-29 cells the differences in fold change in VAF were more minor between the untreated and treated conditions compared to H3122 cells, although a decreasing trend in frameshift mutation allele frequency and increase in unmodified allele frequency were observed upon knockout of each ERBB receptor.

Ten most frequent alleles with a frameshift mutation were chosen from each untreated control sample and the difference in frameshift mutation allele frequency between untreated and treated cells was compared by Wilcoxon signed-rank test. A p-value below 0.05 was considered to indicate statistically significant difference. The frameshift mutation allele frequency showed statistically significant decrease in crizotinib-treated H3122 cell pools with *EGFR*, *ERBB2* and *ERBB3* knockout ($p = 0.0020$, $p = 0.0195$ and $p = 0.0371$, respectively) (**Figure 8B**). The most marked decrease was observed in *EGFR*-knockout cell pool. In HT-29 cells, only *ERBB2* knockout led to statistically significant decrease in frameshift mutation allele frequency upon combination treatment with dabrafenib and trametinib ($p = 0.0371$).

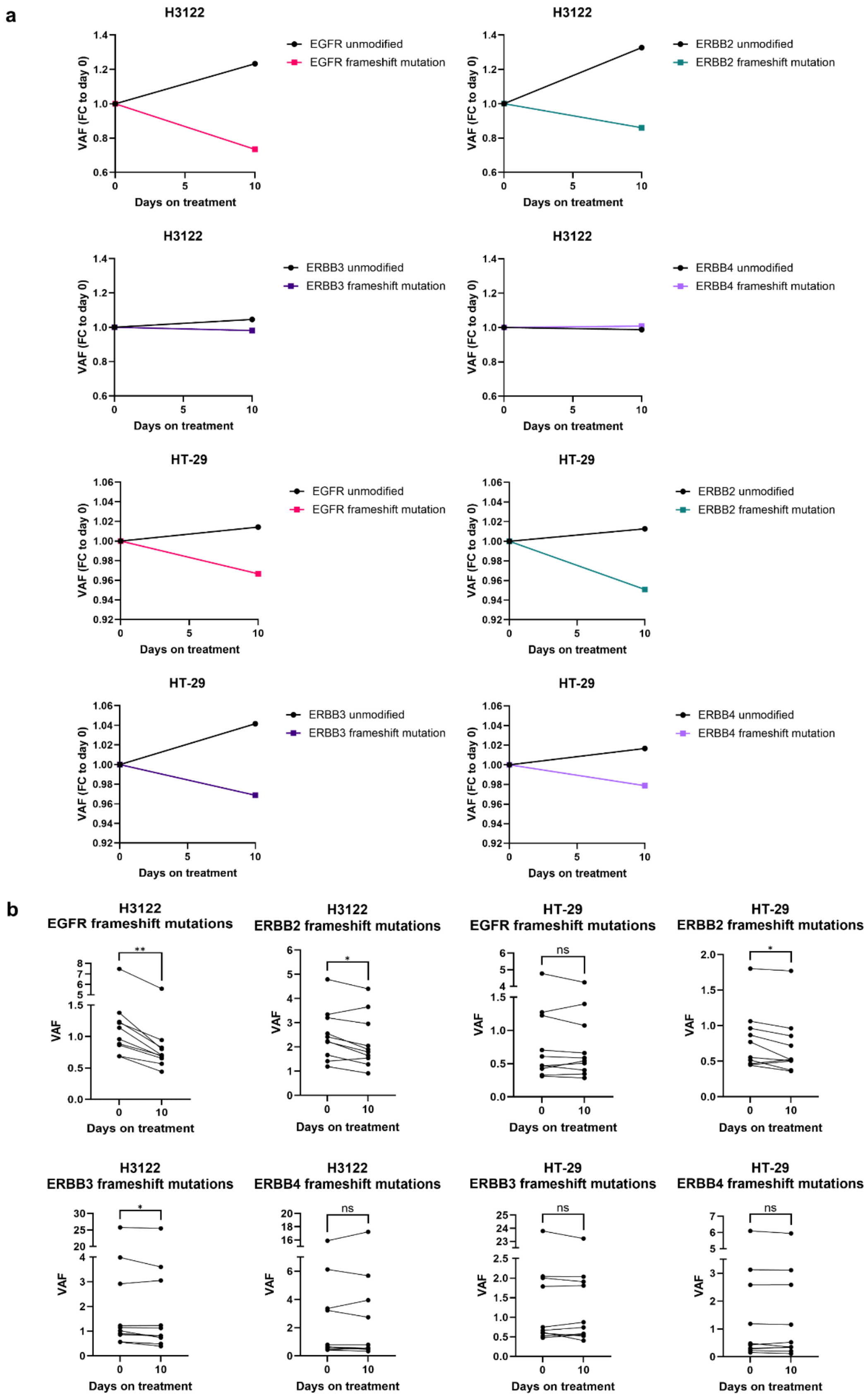

Figure 8. The necessity of ERBB receptors for drug-tolerant H3122 and HT-29 cells. ERBB receptors were knocked out separately by CRISPR-Cas9 in H3122 and HT-29 cell lines and the cells were treated with targeted therapies (H3122: 1 µM crizotinib and HT-29: 1 µM dabrafenib + 10 µg/ml

cetuximab) for 10 days. Genomic DNA from the cells was extracted, the region targeted by CRISPR-Cas9 was amplified by PCR and the PCR products were sequenced by next-generation sequencing. **a**, The fold change in the frequency of unmodified and frameshift mutation alleles to day 0 of treatment was plotted against the time on treatment. **b**, The change in VAF upon drug treatment from ten most frequent alleles containing a frameshift mutation was analyzed by Wilcoxon signed-rank test. *p < 0.05 and **p < 0.01.

In conclusion, the CRISPR knockout efficiency was not ideal and, consequently, the decrease in ERBB frameshift mutation allele frequencies was not drastic. Still, statistically significant decrease in frameshift mutation allele frequency in *EGFR*, *ERBB2* and *ERBB3* knockout cell pools was observed in H3122, which is in line with the increased activation of these receptors observed upon treatment of wild-type H3122 cells. In addition, statistically significant reduction in *ERBB2* frameshift mutation alleles correlates with the strong activation of ERBB2 observed in wild-type HT-29 upon treatment with dabrafenib and cetuximab. These results suggest an important role of signaling through ERBB2 in drug-tolerant HT-29 cells as well as EGFR, ERBB2 and ERBB3 in drug-tolerant H3122 cells. Out of these receptors the H3122 cells were most dependent on EGFR.

3 Discussion

Exogenous NRG1 has been linked to resistance to targeted therapies in different cancer contexts (Cheng et al., 2015; Wilson et al., 2012). The results from our group also demonstrate how many oncogene-addicted cancer cell lines are rescued from targeted therapy treatment by exogenous NRG1. Additional data further demonstrates that treating cancer cell lines with targeted therapies and in absence of exogenous NRG1 leads to increased expression of NRGs and their receptors in autocrine fashion (Takala, 2022). Ultimately, this thesis aimed to determine the functional relevance of upregulation of NRGs and their receptors in drug-tolerant cells. The first aim was to study activation of ERBB receptors and downstream signaling upon treatment with SOC targeted therapies to observe if the increased gene expression correlates with increased protein and activation levels. The second aim was to study the necessity of the ERBB receptors to the survival of the drug-tolerant cells.

To achieve the first aim, oncogene-addicted cancer cell lines were treated with SOC targeted therapies for 10 days. Additionally, 30-day long treatments were included to study the change in the ERBB signaling activation over a longer time period as the drug-tolerant cells evolved. Marked reactivation of RAS/RAF/MEK/ERK and PI3K/AKT downstream signaling pathways was observed in every treated cell line excluding BT-474. Correlating with the reactivation of these downstream signaling pathways, H3122 and HT-29 cells demonstrated the most robust activation of ERBB receptors EGFR and ERBB2 as well as ERBB3 in the case of H3122 cells. To achieve the second aim, ERBB receptors were knocked out in these two cell lines to investigate if signaling through the receptors upregulated upon the drug treatment is crucial for the survival of the drug-tolerant cells. The results from the knockout experiments imply the importance of EGFR, ERBB2 and ERBB3 receptors for drug-tolerant H3122 cells and ERBB2 for drug-tolerant HT-29 cells.

According to the first hypothesis, activation of the NRG/ERBB axis would be a universal resistance mechanism occurring in oncogene-addicted cancers with different driver mutations and different tissue of origin. However, marked upregulation of ERBB receptors was not seen in all investigated cell lines, which would indicate that rather being universal resistance mechanism across different oncogene-addicted cancers, ERBB signaling would be more crucial in certain cancer contexts, including *ALK*-positive NSCLC and *BRAF*-mutated colorectal cancer.

Interestingly, after robust reactivation on day 10 of treatment, the ERBB receptor activation diminished in H3122 and HT-29 cells between days 20 and 30 of treatment. This could imply that the drug-tolerant cells begin to rely on signaling through receptors alternative to ERBBs during the evolution of the drug-tolerant cells. As the activation of AKT and ERK remained relatively high in both H3122 and HT-29 cells on day 30, it would be likely that the alternative receptors would also activate the PI3K/AKT and RAS/RAF/MEK/ERK downstream signaling pathways.

According to the second hypothesis, the drug-tolerant cells upregulating the ERBB signaling axis could not survive under drug exposure without these upregulated ERBB receptors. The results from the knockout experiments show how in H3122 cells the receptors that demonstrated notably increased activation in the drug-tolerant cells, including EGFR, ERBB2 and ERBB3, seemed to have functional relevance as was expected. In HT-29 cells the most prominent reactivation was observed in ERBB2, which also demonstrated to be important to the drug-tolerant cells. However, although notable reactivation of EGFR was detected as well, this receptor did not appear to be relevant for drug-tolerant HT-29 cells in this experimental setup.

3.1 Significance of NRG/ERBB signaling to drug tolerance in different oncogene-addicted cancer contexts

3.1.1 *HER2*-amplified breast cancer

In the *HER2*-amplified breast cancer cell line, BT-474, only slight reactivation of the downstream signaling pathways was observed. The most notable reactivation was observed in the RAS/RAF/MEK/ERK pathway during the experiment where the cells were treated for a total of 30 days. No signs of reactivation of the ERBB receptors were observed. Previously, BT-474 has been reported to be completely rescued from lapatinib by exogenous NRG1 (Wilson et al., 2012). In the same study, BT-474 was treated with 1 µM lapatinib with or without 50 ng/ml NRG1 for 2 h. With lapatinib alone no phosphorylated AKT or ERK is detected but in combination with NRG1 phosphorylation of AKT, ERBB3 and ERBB4 are observed. A similar experiment was also performed using another *HER2*-amplified cell line, AU565. No AKT or ERK activation is detected when treating the cells with lapatinib alone and activation of AKT but not ERK is observed upon combination treatment with lapatinib and NRG1 (Wilson et al., 2012). However, in the study they did not report experiments with a longer treatment period.

Previous results from our group report increased expression of *ERBB3*, *ERBB4* and all *NRGs* in BT-474 upon 10-day lapatinib treatment (Takala, 2022). Based on this and the capability of NRG1 to rescue BT-474 from sensitivity to lapatinib, reactivation of ERBB3 and ERBB4 in drug-tolerant BT-474 cells upon treatment with lapatinib would have been expected. Nevertheless, the level of all activated ERBB receptors diminished after beginning the treatment and remained down until the end of the 30-day treatment period.

Nevertheless, a slight increase in total ERBB3 level on day 1 of treatment relative to untreated control was observed. An increasing trend in the overall ERBB3 level has been previously reported upon 1 μM lapatinib treatment for 48 h, where the overall ERBB3 level began to increase from the timepoint 4 h onwards (Garrett et al., 2011). The modest increase in ERBB3 level on day 1 of treatment observed in this thesis aligns with the referenced study. Still, as the total ERBB3 level decreased between days 1 and 10 followed by continuous decrease thereafter, it would seem that the ERBB3 upregulation is not a sustained effect.

In the same study, immunoprecipitation to isolate ERBB3 following western blot analysis results in detection of increased phosphorylation of ERBB3 on Tyr1197 at 24 h of the treatment. However, the other used anti-phospho-ERBB3 antibodies detecting phosphorylation on Tyr1222 and Tyr1289 only resulted on visible bands on timepoint 0 (Garrett et al., 2011). The antibody used to detect phosphorylated ERBB3 in this thesis recognizes phosphorylated Tyr1289. It could be possible that the sites other than Tyr1289 are phosphorylated in the drug-treated samples and, therefore, the choice of antibody affected that only little phosphorylated ERBB3 was detected in the drug-treated samples. Another possible explanation for the lack of activated ERBB3 detected would be that the receptor remained in the inactive form in the absence of activating stimuli. It would be interesting to test other antibodies detecting phosphorylated ERBB3, including phosphorylation on Tyr1197, to see if more phosphorylated ERBB3 could be detected.

3.1.2 *EGFR*-mutated NSCLC

Although reactivation of PI3K/AKT and RAS/RAF/MEK/ERK downstream signaling pathways, marked activation of ERBB receptors upon SOC targeted therapy treatment was not observed in the NSCLC cell line HCC827 with *EGFR* exon 19 deletion. Interestingly, according to the previous RT-qPCR data from our group, HCC827 cells upregulate the expression of *ERBB2*, *ERBB3* and *ERBB4* upon osimertinib treatment (Takala, 2022). Although the upregulation did not result in increased receptor activation, the upregulated expression of

ERBB2 correlates with the increased overall ERBB2 abundance in the treated cells. Increase in the total ERBB3 level was also observed on day 1 of the treatment correlating with the increase in *ERBB3* expression but on day 10 the abundance was diminished relative to day 1.

Several factors could explain why the increased *ERBB* expression does not correlate with increased receptor activity. The receptor could be degraded rapidly before becoming activated or low levels of ligands could contribute to decreased activation of the receptor. In the case of ERBB3, the translation of the mRNA could be repressed on day 10 leading to lower total ERBB3 abundance than could be expected based on the previous gene expression data.

Others report how HCC827 and another NSCLC cell line with *EGFR* exon 19 deletion, PC9, are not rescued from targeted therapy by exogenous NRG1. Additionally, treatment of PC9 with erlotinib alone or in combination with NRG1 does not lead to activation of ERBB3, AKT or ERK in either condition (Wilson et al., 2012). Furthermore, overexpression of NRG1 in HCC827 cells that are treated with erlotinib does not induce resistance to the treatment (Wilson et al., 2015). All things considered, it seems that HCC827 does not properly activate the NRG/ERBB signaling axis, which could be the reason why it is not rescued from the treatment by exogenous NRG1.

3.1.3 *BRAF* V600E -mutated melanoma

Overall, the activation of ERBB receptors in *BRAF* V600E -mutated melanoma cell line A375 was very minimal. Previously, A375 cells have been shown to be partially rescued from BRAF inhibition by vemurafenib when exposed to exogenous NRG1 (Wilson et al., 2012). Marked elevation on total ERBB2 level was observed on days 10 and 20 of treatment in A375 cells, which correlates with the previous work in our group demonstrating upregulation of *ERBB2*, *ERBB3* and *ERBB4*, as well as *NRG3* in A375 upon combination treatment with dabrafenib and trametinib (Takala, 2022).

Slightly elevated overall ERBB3 level was also detected on day 1 of treatment relative to the untreated control. In literature upregulation of ERBB3 upon BRAF inhibition has been reported: Treating *BRAF*-mutated melanoma cell lines WM115 (V600D mutation) and 1205Lu (V600E mutation) with vemurafenib overnight leads to increase in total ERBB3 level compared to untreated control in both cell lines. Additionally, 1205Lu cells increase *ERBB3* expression in the same experimental setup. In A375 cells, the ERBB3 expression on the cell surface analyzed by flow cytometry is increased upon overnight vemurafenib treatment compared to DMSO control (Abel et al., 2013).

The necessity of ERBB3 to drug-treated *BRAF*-mutant melanoma cell lines has been investigated before. In one study, ERBB3 was blocked with an antibody, huHER3-8, in 1205Lu, M238 (*BRAF* V600E -mutated melanoma) and A375 cells treated with vemurafenib. The cells were further stimulated with NRG1 before western blot analysis revealing ablation of AKT activation by the ERBB3-targeting antibody. The cytotoxicity of the vemurafenib and anti-ERBB3 antibody combination was also assessed. Cell death is induced upon ERBB3-blocking in vemurafenib-treated and NRG1-stimulated cells to the same level as in vemurafenib-treated cells. As blocking of ERBB3 in vemurafenib-treated cells that were not stimulated by NRG1 does not induce cell death compared to cells treated with vemurafenib as single agent, the authors suggest that the basal ERBB3 activation does not affect survival of the cells (Kugel et al., 2014).

In this thesis, the activation of ERBB3 in treated A375 cells was very low, which would support the idea that ERBB3 does not have a major role in the survival of the cells. The activation of ERBB2 was also low in the cells although pronounced elevation of total ERBB2 abundance was observed. Considering the observed ERBB2 dependence of the colorectal cancer cell line HT-29 harboring the same *BRAF* mutation as A375 cell line, it could be interesting to further study the importance of ERBB2 for drug-tolerant A375 cells.

3.1.4 *ALK*-positive NSCLC

Increased activation of EGFR, ERBB2 and ERBB3 was observed in *ALK*-positive NSCLC cell line H3122 upon crizotinib treatment. These receptors were also demonstrated to be important to the treated cells by the *ERBB* knockout study. Previous reports also describe the importance of NRG receptors, as H3122 is completely rescued from ALK-inhibitor TAE684 sensitivity by exogenous NRG1 (Wilson et al., 2012). Similarly, overexpression of NRG1 by introducing open reading frame of NRG1 into H3122 cells increases the viability of the cells upon treatment with either crizotinib or TAE684 (Wilson et al., 2015). The observed reactivation of ERBB2 and ERBB3 also aligns with the previous data from our group that demonstrates increased expression of *ERBB2*, *ERBB3*, *ERBB4*, *NRG1* and *NRG4* in H3122 cells upon crizotinib treatment (Takala, 2022). *EGFR* is not upregulated upon the treatment (Takala, 2022), which would suggest that the reactivation of the receptor is due to post-translational regulation, such as decreased level of degradation.

Bypass signaling through EGFR has been well characterized as a resistance mechanism in *ALK*-rearranged NSCLC. EGFR activation by crizotinib has been reported in crizotinib-resistant H3122 cell line established by continuous exposure to increasing concentrations of crizotinib. The activation is reported to be likely through non-genomic mechanism and the cells regain their sensitivity upon discontinuation of the drug treatment (Yamaguchi et al., 2014). In another study, increased EGFR as well as ERBB2 and ERBB3 activation is observed in TAE684-resistant H3122 cell line compared to treatment naïve cells after 6 h treatment with TAE684 (Tanizaki et al., 2012). Furthermore, in patient samples of crizotinib-resistant *ALK*-positive NSCLCs, the EGFR activation is increased compared to crizotinib-sensitive samples collected before starting crizotinib therapy in four out of nine samples (Katayama et al., 2012).

In this thesis, H3122 cells demonstrated the greatest dependence on EGFR out of all ERBB receptors. As EGFR signaling has already been established as a resistance mechanism in this cancer context, the result highlights the validity of our experimental setup for investigating the dependence of the drug-tolerant cells on the ERBB receptors.

In addition to the aforementioned studies, exogenous EGFR ligands EGF, TGF-α and HB-EGF have been shown to reduce crizotinib-sensitivity in *ALK*-rearranged lung cancer cell lines including H3122. This is suggested to occur in paracrine manner as coculture of the cancer cells with epithelial cells expressing EGFR-ligands increases H3122 cell viability upon 72 h crizotinib treatment. In the same study EGF, TGF-α and HB-EGF levels from the cell culturing medium of H3122 cells were measured after 48 h of culturing the cells and the levels are very low (Yamada et al., 2012). The EGFR activation level in untreated H3122 cells was low supporting the data from this study by Yamada et al. However, EGFR being reactivated on days 10 and 20 of the crizotinib-treatment in H3122 cells cultured alone indicates that H3122 cells do produce EGFR ligands under the drug treatment and activate the receptors in autocrine manner.

In addition to EGFR, the role of ERBB2 and ERBB3 in drug tolerance to ALK inhibition can be supported by the results of this thesis. Signaling through ERBB2/ERBB3 heterodimer as a mechanism to resistance is also suggested by a previous study where *ALK*-rearranged cell lines H3122, H2228 and MGH006 were treated for five days with recombinant NRG1 and TAE684. The recombinant NRG1 promotes resistance to the drug in these cell lines but this effect of NRG1 is lost if the cells are treated with TAE684 and lapatinib in combination (Wilson et al., 2015). In the referenced study the cells were stimulated with exogenous NRG1. Therefore, the results of this thesis provide new insights into the importance of ERBB2 and ERBB3 receptors in drug-tolerant cells that are not influenced by stimulation with exogenous NRG1. Furthermore, it would be interesting to attempt blocking ERBB2 and/or ERBB3 in combination with ALK inhibition without stimulating the cells with NRG1 to investigate if the combination would affect the viability of the drug-tolerant cells.

3.1.5 *BRAF* V600E -mutated colorectal cancer

According to previous work in our group, *ERBB2*, *ERBB3* and *ERBB4* as well as *NRG4* are notably upregulated upon SOC targeted therapy treatment in *BRAF* V600E -mutated colorectal cancer cell line HT-29 (Takala, 2022). Reactivation of ERBB2 in HT-29 cells observed in this thesis correlates with this previous data. Interestingly, EGFR but not ERBB3 activation was enhanced in this cell line in the drug-tolerant cells. Similarly to H3122 cells, this would indicate that the reactivation of EGFR would be caused by decreased level of receptor degradation rather than changes in the level of gene transcription. Also, the lack of ERBB3 activation could be explained by rapid degradation of the receptor before being activated or, alternatively, lack of activating stimulus.

Increase in ERBB3 signaling in *BRAF*-mutated colon or colorectal cancer upon vemurafenib treatment has been reported previously by several others. 48 h treatment with vemurafenib leads to elevated *ERBB3* expression and total protein level in *BRAF* V600E -mutated colon cancer stem cells. In addition, exogenous NRG1 increases proliferation of the *BRAF* V600E -mutated colon cancer stem cells in a dose-dependent manner in cells treated with vemurafenib for 5 days compared to vemurafenib treatment alone (Prasetyanti et al., 2015). In another study, *BRAF* V600E colorectal adenocarcinoma cell line, COLO-201, was treated with vemurafenib alone or in combination with NRG1 and activation of ERBB3 and AKT is only able to be detected with cotreatment of vemurafenib and NRG1 (Wilson et al., 2012). In this thesis, the total ERBB3 abundance slightly increased relative to the untreated control on days 1 to 20 similarly to what was seen in the study by Prasetyanti et al. In the study they did not assess the amount of phosphorylated receptor and the results of this thesis point to increased total ERBB3 abundance not translating to more activation of the receptor. As the study by Wilson et al. also reports activation of ERBB3 and AKT only upon NRG1 stimulation, likely exogenous NRG1 would be required to see a robust activation of the ERBB3 receptor.

The same study by Prasetyanti et al. also investigated the effect of *ERBB3* expression silencing and ERBB3 blocking by an antibody in the *BRAF* V600E mutant colon cancer stem cell lines.

They treated the cells with silenced or blocked ERBB3 with combination of NRG1 and vemurafenib and observed a lower proliferation in these groups compared to control where the ERBB3 was not blocked or silenced. If the ERBB3-silenced cells and control cells were treated with vemurafenib alone, the effect is not as prominent, which again indicates that the exogenous NRG1 is important to these cells (Prasetyanti et al., 2015).

Very robust activation of ERBB2 was observed in the drug-tolerant HT-29 cells and the CRISPR-sequencing result supported the importance of the ERBB2 receptor to the drug-tolerant cells. Based on this, targeting ERBB2 in addition to BRAF and EGFR in *BRAF*-mutated colorectal cancer could potentially be an effective treatment combination in the clinic. This could also be achieved by combining a BRAF inhibitor with a pan-ERBB inhibitor targeting all ERBBs excluding the pseudokinase ERBB3. This combination has been evaluated in colorectal cancer cell lines, of which the ones with high basal levels of ERBB2 have been shown to respond better to vemurafenib and pan-ERBB inhibitor afatinib combination treatment compared to cell lines expressing ERBB2 on lower levels, which suggest that ERBB2 expression status could be used to determine, which patients could benefit from the vemurafenib and afatinib treatment combination (Miele et al., 2020).

3.2 Possible sources of error and study limitations

3.2.1 ERBB signaling activation experiments

The ERBB receptors are similar in structure and size. It is possible that the primary antibodies used to detect the receptors by western blot may cross-react with other ERBBs increasing risk to inaccurate interpretation of the results. A strong EGFR protein expression was observed in the *EGFR*-mutant HCC827 cell line. In the total and phosphorylated ERBB4 blots the band observed right below 180 kDa marker in the untreated sample could be caused by cross-reaction of the primary antibody with EGFR (175 kDa in size) instead of ERBB4 (180 kDa in size). Similarly, BT-474 cell line expresses high levels of ERBB2 due to the gene amplification. Strong band slightly above the 180 kDa marker in the phosphorylated and total ERBB4 blots in the untreated control sample is likely result of the primary antibody cross-reacting with the overexpressed ERBB2 (185 kDa in size) rather than binding the actual ERBB4.

In this study the levels of NRGs or other ERBB receptor ligands produced by the treated cells were not measured. Even though the activation of ERBB receptors indicates the presence of ligands, it would have been meaningful to investigate if the upregulation of the NRGs reported by the previous work in our group translates to increased NRGs on the protein level. However, the detection of NRGs was not possible as no NRG-targeting antibodies that would be adequately characterized are available (Montero et al., 2008).

3.2.2 ERBB receptor dependency experiments

The differences in frameshift mutation allele frequencies between the untreated and treated conditions appeared to be small although statistically significant. This could be explained by the overall low knockout efficiency in H3122 and HT-29 cells. The nucleofection efficiency in T47D was determined to be low and it can be expected that the low knockout efficiency in H3122 and HT-29 cells is also largely due to the poor nucleofection efficiency. The poor nucleofection efficiency results in fewer cells with a homozygous knockout. Homozygous knockout would be required to observe a drop in the frameshift allele frequency upon treatment assuming that the receptor is crucial for the survival of the cells. Knockout studies in mice demonstrate how homozygous knockout of *EGFR*, *ERBB2* or *ERBB3* is required to observe the developmental deficits caused by lack of the receptors (Erickson et al., 1997; Lee et al., 1995; Miettinen et al., 1995). Similarly here, the cancer cells with a heterozygous ERBB receptor knockout would be expected to not be affected by the lack of one of the *ERBB* alleles.

Therefore, low nucleofection and thus low knockout efficiency in this experimental setup could lead to biologically significant receptors being missed. This is because not enough homozygous knockout cells are present in the knockout cell pool so statistically significant difference in the frameshift allele frequency cannot be detected between the untreated and treated sample. Considering this, the statistically significant differences reported, although being small, could indicate biological significance of the receptors to the drug-tolerant cells. Additionally, as notably increased activation of EGFR was observed in wild-type HT-29 drug-tolerant cells, it would have been expected to observe a reduction in *EGFR* frameshift allele frequency over the course of the treatment in the knockout cell pool. Here, it could be possible that the low knockout efficiency in HT-29 cells would be the reason why such reduction was not observed. Therefore, further studies would be needed to assess the significance of EGFR to the drug-tolerant HT-29 cells.

Another limitation to the study is the lack of additional control consisting of CRISPR-treated cells that are cultured for the whole duration of the drug-treatment (10 days) in absence of the drug. This control would have been important to show that the proportion of knockout cells does not decrease itself by time and that the decrease is indeed caused by the effect of drugs.

It would be worthwhile to repeat the knockout experiments including the additional untreated control cells cultured as long as the drug-treated cells. Still, more important would be to overcome the low knockout efficiency mainly including the issues with the low nucleofection efficiency. Additionally, cell lines with homozygous ERBB receptor knockout could be produced and used for the experiments. This would exclude the influence of the knockout efficiency on the results. The use of knockout cell lines would also enable the use of cell viability tests to investigate if the viability of the drug-tolerant knockout cells is decreased compared to the wild-type cells by the drug treatment.

3.3 Conclusion and future directions

The results of this thesis indicate the importance of ERBB2 and ERBB3 to drug-tolerant H3122 cells as well as highlight the already established role of EGFR in drug resistance in *ALK*-rearranged NSCLC. The results also demonstrate the importance of ERBB2 to drug-tolerant HT-29 cells.

These results contribute to understanding the behavior of drug-tolerant cell populations and the evolution of the ERBB signaling in these cells over a longer time-period. Discovering the pathways crucial for the viability of these drug-tolerant cells can enable finding more effective treatment strategies to possibly eradicate these cells. Based on the results of this thesis it could be suggested that targeting EGFR, ERBB2 and ERBB3 in addition to ALK inhibition might benefit the patients with *ALK*-positive NSCLC and hinder the resistance development. Also, targeting ERBB2 in addition to EGFR and BRAF in *BRAF*-mutated colorectal cancer could be more effective than the current SOC. Effectiveness of pan-ERBB inhibitors in combination with the drug targeting the oncogenic driver mutation could also be evaluated as possible treatment combination in treatment of these two cancers. All in all, more studies are required to validate the potential of these treatment combinations in the clinic.

4 Materials and methods

4.1 Cell culture

EBC-1, H3122, HCC827, HT-29 and T47D cells were cultured in RPMI 1640 medium (Euroclone, cat. no. ECB9006L), whereas A375 and BT-474 cells were cultured in DMEM (Euroclone, cat. no. ECB7501L). Both cell culture mediums were supplemented with 10 % fetal bovine serum (Biowest, cat. no. S181B), 1 % penicillin-streptomycin (Euroclone, cat. no. ECB3001D) and 1 % L-glutamine (Euroclone, cat. no. ECB3004D). In addition, the medium for T47D cells contained 0.01 mg/ml human insulin (Merck, cat. no. I9278-5ML). All cell lines were sustained in a humidified incubator with 5 % CO_2 level and +37 °C temperature. The cells were passaged to new cell culture plates once reaching 80 % confluency using trypsin (Thermo Fisher Scientific, Gibco™, cat. no. 25-200-072).

4.2 *ERBB* knockouts using CRISPR and nucleofection

The necessity of the ERBB receptors for the survival of drug-tolerant cells was studied by knocking out the ERBB receptors separately. CRISPR-Cas9 using RNP and nucleofection to deliver the RNP into the cells was used to produce the knockout cell pools.

4.2.1 RNP complex assembly

To produce a complete gRNA, crRNA (Appendix 2 - crRNA sequences) and tracrRNA (Integrated DNA Technologies (IDT), cat. no. 1073190) solutions were mixed 1:1 in a PCR tube (Table 1), which was then incubated at +95 °C for 5 min. Thereafter, the solutions were let to cool at room temperature (+20-25 °C). Next, Alt-R™ S.p. Cas9 Nuclease V3 (IDT, cat. no. 1081059) was diluted in Cas9 working buffer (20 mM HEPES, 150 mM KCl, 1 mM $MgCl_2$, 10% glycerol and 1 mM TCEP) and added to the crRNA:tracrRNA solution by slowly pipetting. The solution was incubated for minimum of 20 min at room temperature for RNP complex assembly.

Table 1. The components for preparation of crRNA:tracrRNA solution (left column) and RNP complexes (right column). The volumes are per one reaction.

crRNA:tracrRNA solution	RNP complexes
2.6 µl Cas9 working buffer	3.36 µl Cas9 working buffer
1.2 µl 100 µM crRNA diluted in IDT Nuclease-Free Duplex buffer (cat. no. 1072570)	1.64 µl Alt-R™ S.p. Cas9 Nuclease V3
1.2 µl 100 µM tracrRNA	5 µl crRNA:tracrRNA solution

4.2.2 Nucleofection

The cells to be nucleofected were detached using trypsin and pelleted by 5 min centrifugation at 300 rcf. The cell pellet was resuspended in suitable Nucleofector® solution (Table 2). Then, 20 µl of the cell suspension was added to a PCR tube containing 10 µl of the RNP complex solution prepared in section 4.2.1 and mixed well by pipetting. 20 µl of the solution was transferred to a well of Nucleocuvette® strip and the nucleofection was performed using the X Unit of 4D-Nucleofector® system from Lonza. To determine nucleofection efficiency, 0.5 µl of pmaxGFP™ plasmid (Lonza, cat. no. V4XC-1032) encoding GFP was nucleofected alone in a separate reaction. After nucleofection, the cells were let to sit in the Nucleocuvette® strip for 10 min to increase the nucleofection efficiency. Thereafter, 100 µl of cell culture medium was added to each well and cells were transferred to a well of 6-well plate containing 2 ml of cell culturing medium.

Table 2. Nucleofection conditions for each cell line including the number of nucleofected cells per one reaction, nucleofector solution and program.

Cell line	**Number of cells per one reaction**	**Nucleofector solution**	**Nucleofector program**
T47D	400 000	SE (Lonza, cat. no. V4XC-1032)	EN-104
H3122	400 000	SE (Lonza, cat. no. V4XC-1032)	CA-137
HT-29	300 000	SF (Lonza, cat. no. V4XC-2032)	FF-137

4.2.3 Post-nucleofection

The newly nucleofected cells were incubated in a humidified incubator at 5% CO_2 and +37 °C for minimum of 48 h. Thereafter, the cells were either passaged onto larger cell culture dishes in order to grow enough cells for 10-day drug treatments described in section 4.3.3 or the cells were used for preparing samples for western blotting as described in 4.4.1. The cells nucleofected with pmaxGFP™ plasmid were imaged 24 h post-nucleofection using bright-field and fluorescence imaging with EVOS M5000 Imaging System from Thermo Fisher Scientific.

4.3 10- and 30-day drug treatments with SOC targeted therapies

To study ERBB receptor and downstream signaling activation, oncogene-addicted cancer cell lines were treated for 10- and 30-days with SOC targeted therapies. In addition, to study the necessity of the ERBB receptors for the viability of drug-tolerant cells, ERBB receptor knockout cell pools (section 4.2) were treated with the SOC targeted therapies for 10 days.

4.3.1 10-day treatment of wild-type oncogene-addicted cancer cells

The cells were seeded on cell culturing dishes of 10 cm or 15 cm in diameter as listed in Table 3. One day post-seeding, the drug treatments were started. The drugs and drug concentrations used for each cell line are listed in Table 4. The drugs (excluding cetuximab) were first diluted in DMSO to reach a concentration of 1 mM before mixing them to the cell culture medium to reach the final drug concentration. DMSO with a final concentration of 14 mM was used for the control cells. Before adding the new drug medium, the old cell culture medium was removed, and the cells were washed with PBS (Thermo Fisher Scientific, GibcoTM, cat. no. 10010-015).

Table 3. The number of cells seeded per dish for 10-day SOC targeted therapy treatments in wild-type oncogene-addicted cancer cell lines. The cells were seeded on cell culturing dishes, which were either 10 cm or 15 cm in diameter. One dish was used per condition.

Cell line	**Number of cells seeded per dish**		
	Control	**24-h treatment**	**10-day treatment**
A375 Melanoma with *BRAF* V600E point mutation	300 000 cells/ 10 cm dish	300 000 cells/ 10 cm dish	5 000 000 cells/ 15 cm dish
BT-474 Breast cancer with *HER2* amplification	700 000 cells/ 10 cm dish	700 000 cells/ 10 cm dish	5 000 000 cells/ 10 cm dish
EBC-1 NSCLC with *MET* amplification	500 000 cells/ 10 cm dish	500 000 cells/ 10 cm dish	3 500 000 cells/ 15 cm dish
H3122 NSCLC with *ALK* fusion	500 000 cells/ 10 cm dish	500 000 cells/ 10 cm dish	2 000 000 cells/ 15 cm dish
HCC827 NSCLC with *EGFR* del19	800 000 cells/ 10 cm dish	800 000 cells/ 10 cm dish	2 000 000 cells/ 15 cm dish
HT-29 Colorectal cancer with *BRAF* V600E point mutation	500 000 cells/ 10 cm dish	500 000 cells/ 10 cm dish	3 000 000 cells/ 15 cm dish

Table 4. The SOC targeted drug treatments used for each cell line. Same drugs and drug concentrations were used in experiments described in sections 4.3.1, 4.3.2 and 4.3.3.

Cell line	**Treatment**	**Drug target**
A375 Melanoma with *BRAF* V600E point mutation	1 µM Dabrafenib (MedChemExpress, cat. no. HY-14660) + 100 nM Trametinib (Selleck Chemicals, cat. no. S2673)	BRAF and MEK
BT-474 Breast cancer with *HER2* amplification	1 µM Lapatinib (Cayman Chemical, cat. no. 11493)	HER2
EBC-1 NSCLC with *MET* amplification	1 µM or 100 nM Crizotinib (Tocris Bioscience, cat. no. 4368)	MET
H3122 NSCLC with *ALK* fusion	1 µM Crizotinib (Tocris Bioscience, cat. no. 4368)	ALK
HCC827 NSCLC with *EGFR* del19	1 µM Osimertinib (Cayman Chemical, cat. no. 16237)	EGFR
HT-29 Colorectal cancer with *BRAF* V600E point mutation	1 µM Dabrafenib (MedChemExpress, cat. no. HY-14660) + 10 µg/ml Cetuximab (Merck, Erbitux®, stock concentration 5 mg/ml)	BRAF and EGFR

Samples for western blotting (section 4.4.1) were prepared from the cells on control and 24-h treatment dishes 24 h after beginning the drug treatment. Furthermore, western blotting samples from the cells on the 10-day treatment dish were prepared 10 days after beginning the treatment, and the drug medium for these cells was changed to fresh one on the fifth day of the treatment.

4.3.2 30-day treatment of wild-type oncogene-addicted cancer cells

The cells were seeded on cell culturing dishes of 10 and 15 cm in diameter as described in Table 5. The drug treatment was started one day after seeding and was performed the same way as described in section 4.3.1. The drug medium was changed to fresh one every 3-4 days. Western blotting samples (section 4.4.1) were prepared from the control and 24-h treated cells 24 h after starting the drug treatment and from cells treated for longer the samples were prepared at their given timepoint (Table 5). Before lysing the cells, they were counted using Bio-Rad TC10™ automated cell counter.

Table 5. The number of cells seeded per dish for 30-day treatment of wild-type oncogene-addicted cancer cell lines. Cell culturing dishes of 10 or 15 cm in diameter were used and the cells were seeded on two dishes per condition.

Cell line	**Number of cells seeded per dish**				
	Control	**24-h treatment**	**10-day treatment**	**20-day treatment**	**30-day treatment**
A375 Melanoma with *BRAF* V600E point mutation	300 000 cells/ 10 cm dish	300 000 cells/ 10 cm dish	5 000 000 cells/ 15 cm dish	5 000 000 cells/ 15 cm dish	5 000 000 cells/ 15 cm dish
BT-474 Breast cancer with *HER2* amplification	700 000 cells/ 10 cm dish	700 000 cells/ 10 cm dish	5 000 000 cells/ 10 cm dish	5 000 000 cells/ 15 cm dish	5 000 000 cells/ 15 cm dish
H3122 NSCLC with *ALK* fusion	500 000 cells/ 10 cm dish	500 000 cells/ 10 cm dish	2 000 000 cells/ 15 cm dish	2 000 000 cells/ 15 cm dish	2 000 000 cells/ 15 cm dish
HCC827 NSCLC with *EGFR* del19	800 000 cells/ 10 cm dish	800 000 cells/ 10 cm dish	2 000 000 cells/ 15 cm dish	2 000 000 cells/ 15 cm dish	2 000 000 cells/ 15 cm dish
HT-29 Colorectal cancer with *BRAF* V600E point mutation	500 000 cells/ 10 cm dish	500 000 cells/ 10 cm dish	3 000 000 cells/ 15 cm dish	3 000 000 cells/ 15 cm dish	3 000 000 cells/ 15 cm dish

4.3.3 10-day treatment of ERBB receptor knockout cell pools

The cells were seeded for the experiment according to Table 6. The drug treatments were started one day post-seeding and performed the same way as described in section 4.3.1. The cell culture mediums were changed for 10-day treatment dishes on the fifth day after beginning the drug treatments. Genomic DNA was extracted from the cells either 24 h (control cells) or 10 days (drug-treated cells) after beginning the treatment according to the protocol described in section 4.5.1.

Table 6. The number of cells seeded per dish for 10-day treatment of ERBB receptor knockout cell pools. The cells were seeded on cell culturing dishes of 10 or 15 cm in diameter, and one dish was used per condition.

Cell line	**Number of cells seeded per dish**	
	24-h control	**10-day treatment**
H3122 NSCLC with *ALK* fusion	500 000 cells/ 10 cm dish	2 000 000 cells/ 15 cm dish
HT-29 Colorectal cancer with *BRAF* V600E point mutation	500 000 cells/ 10 cm dish	3 000 000 cells/ 15 cm dish

4.4 Western blot

4.4.1 Sample preparation

First, the cells were detached using trypsin and transferred to a falcon tube following centrifugation at 300 rcf for 5 min at +4 °C. The supernatant was removed, and the cells were resuspended in ice-cold PBS and transferred to an Eppendorf tube following centrifugation at 300 rcf for 5 min at +4 °C. PBS was removed and the cells were resuspended in an appropriate volume of lysis buffer (Appendix 1 - Preparation of buffers for western blotting) ranging roughly from 100 to 400 µl depending on the pellet size. Next, the sample was centrifuged at 21 130 rcf for 5 min at +4 °C. The supernatant containing the protein was transferred to a new Eppendorf tube.

Protein concentration in the lysates was determined using Bradford assay. Briefly, the Bio-Rad Protein Assay Dye Reagent Concentrate (cat. no. 5000006) was diluted 1:5 in Milli-Q water. 200 µl of the diluted reagent and 2 µl of lysate was mixed in one well of a 96-well plate. Absorbance was measured using Multiskan FC from Thermo Fisher Scientific. Each sample was measured in duplicates.

After determining the protein concentrations, 6X SDS sample buffer (Appendix 1 - Preparation of buffers for western blotting) was added 1:6 to the lysates and the samples were boiled at +95 °C for 5 min to denature protein.

4.4.2 SDS-page

The components for SDS-page gels are listed in Table 7. First, the components of resolving gel were mixed in a falcon tube and the solution was cast between two glass slides. The resolving gel was let to polymerize for 30 min before the stacking gel and comb were added on top.

Table 7. The components for preparation of SDS-page gels. The given volumes are for preparation of one gel.

Stacking gel		**Resolving gel (8% acrylamide)**	
Milli-Q water	1.525 ml	**Milli-Q water**	3.625 ml
30% acrylamide	325 µl	**30% acrylamide**	2 ml
4xTris-Cl/SDS pH 6.8	625 µl	**4xTris-Cl/SDS pH 8.8**	1.875 ml
10% APS	12.5 µl	**10% APS**	25 µl
TEMED	5 µl	**TEMED**	5 µl

15 to 45 µg of the protein sample was loaded per well. BlueStar Plus Prestained Protein Marker (Nippon Genetics, cat. no. MWP04) was used as the protein size marker. The gel was run at 70 V for 20 min before increasing the voltage to 120 and, thereafter, the gel was let to run for 90 min.

4.4.3 Protein transfer, blocking and imaging of the membranes

Wet tank transfer was performed using Mini Trans-Blot® cell from Bio-Rad and Bio-Rad 0.2 µm nitrocellulose membranes (cat. no. 1620112). Preparations for the protein transfer were performed according to the manufacturer's instructions (Bio-Rad, n.d.). The transfer was carried out at 20 V overnight at +4 °C.

Following protein transfer, the membranes were blocked in 5 % milk powder in Tris-buffered Saline with Tween 20 (TBST) for 1 h following 3 x 5 min washing in TBST (Appendix 1 - Preparation of buffers for western blotting) on a shaker. Incubation with the primary antibodies (Table 8) was performed overnight at +4 °C.

Table 8. Primary antibodies and their dilutions used for western blotting. NaN_3 solution was added to each antibody dilution 1:1000 to increase its storage time. BSA = bovine serum albumin.

Primary antibody	**Dilution**
Anti-pEGFR (Cell Signaling Technology, cat. no. 2220)	1:1000 in 5 % BSA in TBST
Anti-pERBB2 (Cell Signaling Technology, cat. no. 2247)	1:1000 in 5 % BSA in TBST
Anti-pERBB3 (Cell Signaling Technology, cat. no. 4791)	1:1000 in 5 % BSA in TBST
Anti-pERBB4 (Cell Signaling Technology, cat. no. 4757)	1:1000 in 5 % BSA in TBST
Anti-EGFR (Cell Signaling Technology, cat. no. 2232)	1:1000 in 5 % BSA in TBST
Anti-ERBB2 (Invitrogen, cat. no. MA5-14057)	1:2000 in 5 % BSA in TBST
Anti-ERBB3 (Cell Signaling Technology, cat. no. 12708)	1:1000 in 5 % BSA in TBST
Anti-ERBB4 (Cell Signaling Technology, cat. no. 4795)	1:1000 in 5 % BSA in TBST
Anti-ERBB4 (Abcam, cat. no. ab32375)	1:1000 in 5 % BSA in TBST
Anti-pAKT (Cell Signaling Technology, cat. no. 4060)	1:1000 in 5 % BSA in TBST
Anti-AKT (Cell Signaling Technology, cat. no. 2920)	1:1000 in 5 % BSA in TBST
Anti-pERK (Cell Signaling Technology, cat. no. 9101)	1:1000 in 5 % BSA in TBST
Anti-ERK (Cell Signaling Technology, cat. no. 9102)	1:1000 in 5 % BSA in TBST
Anti-β-tubulin (Merck, cat. no. T7816)	1:10 000 in 5 % BSA in TBST

After the overnight incubation with primary antibodies, the membranes were washed in TBST 3 x 5 min following 1 h incubation with the secondary antibodies (Table 9) at room temperature. Thereafter, the membranes were washed again in TBST 3 x 5 min and imaged using Odyssey® CLx from LI-COR Biosciences.

Table 9. Secondary antibodies and their dilutions used for western blotting.

Secondary antibody	**Dilution**
IRDye® 800CW Donkey anti-Rabbit IgG (LI-COR Biosciences, cat. no. 926-32213)	1:15 000 in 5% milk powder in TBST
IRDye® 800CW Donkey anti-Mouse IgG (LI-COR Biosciences, cat. no. 926-32212)	1:15 000 in 5% milk powder in TBST

4.4.4 Stripping

In order to remove bound primary and secondary antibodies before reprobing, the membranes were incubated in stripping buffer (Appendix 1 - Preparation of buffers for western blotting) 3 x 10 min at room temperature following washing in TBST 3 x 5 min. Thereafter, the membranes were re-blocked and incubated together with new primary antibodies as described in section 4.4.3.

4.5 Sample preparation for Next-generation sequencing

Next-generation sequencing was used to determine the proportion of wild-type and *ERBB* knockout cells in CRISPR-treated pool of cells containing wild-type cells, heterozygous and homozygous knockout cells as well as cells with in-frame indels.

4.5.1 DNA extraction

The cells were detached using trypsin, transferred into a falcon tube, and centrifuged for 5 min at 300 rcf. Then, the cells were resuspended in PBS, transferred into an Eppendorf tube, and centrifuged again 5 min at 300 rcf. PBS was removed and DNA extraction was performed using NucleoSpin® Tissue kit from Macherey-Nagel (cat. no. 740952) following the manufacturer's protocol. In brief, the cells were resuspended in 200 µl of buffer T1. 25 µl of Proteinase K and 200 µl of buffer B3 were added and the sample was mixed by vortex. Then, the sample was incubated at +70 °C for 15 min. 210 µl of 99.5 % ethanol was added to the sample and the sample was mixed again by vortex. The whole sample was transferred into NucleoSpin® Tissue Column placed into a collection tube. Then, the sample was centrifuged 1 min at 11 000 rcf and the flow-through was discarded. The membrane was washed first with 500 µl buffer BW and then with 600 µl buffer B5. The sample was centrifuged for 1 min at 11 000 rcf after addition of each washing buffer as well as once after completing the washing steps to dry the membrane. Finally, the DNA was eluted to 100 µl buffer BE and the DNA concentration was determined using NanoDrop ND-1000 Spectrophotometer.

4.5.2 PCR and agarose gel electrophoresis

For the next-generation sequencing, short DNA sequences of 200-250 bp containing the genomic area targeted by CRISPR-Cas9 had to be amplified from the extracted genomic DNA. Primers for this purpose were designed and ordered from Eurofins Scientific (Appendix 3 - PCR primer sequences). The set up for PCR reactions and the PCR cycling conditions are listed in Table 10. All components were assembled in ice before transferring the reaction mixtures into Applied Biosystems™ Veriti™ 96-Well Thermal Cycler.

Table 10. PCR reaction set up (left side) and cycling conditions (right side). The PCR master mix contained Phusion High-Fidelity DNA Polymerase.

Component	Amount
Phusion® Hot Start Flex 2X Master Mix (NEB, cat. no. M0536)	25 µl
Forward primer (10 µM)	2.5 µl
Reverse primer (10 µM)	2.5 µl
Template DNA	150 ng
AccuGENE™ water	To 50 µl

	Step	Temperature	Time
	Initial Denaturation	98 °C	30 s
35 cycles	Denaturation	98 °C	10 s
	Annealing	61 °C	20 s
	Extension	72 °C	10 s
	Final Extension	72 °C	5 min

Following PCR, amplification of the correct DNA sequence was confirmed using agarose gel electrophoresis. Gel with 1% agarose in Tris-acetate-EDTA buffer and 1:25 000 Midori Green Advance DNA stain (Nippon Genetics, cat. no. MG04) was prepared. 5 µl of PCR product was mixed with 1 µl of Gel Loading Dye, Purple (6X) (NEB, cat. no. B7024S) and loaded onto the agarose gel. GeneRuler 100 bp DNA Ladder from Thermo Fisher Scientific (cat. no. SM0241) was used as a DNA size marker. The gel was imaged using ChemiDoc™ MP Imaging System from Bio-Rad. In case additional, undesired DNA sequences were amplified in addition to the correct PCR product, the PCR products were separated by agarose gel electrophoresis from the whole remaining PCR sample.

NucleoSpin® Gel and PCR Clean-up kit from Macherey-Nagel (cat. no. 740609) was used to either purify the PCR product directly or from agarose gel. In brief, 45 µl of the PCR sample was mixed with 90 µl of buffer NTI or in case of purification from agarose gel, 200 µl of buffer NTI was added per 100 mg of gel. The gel was dissolved by incubation at +50 °C for 5-10 min. Then, the whole sample was transferred into NucleoSpin® Gel and PCR Clean-up Column provided in the kit and centrifuged 30 s at 11 000 rcf to bind the DNA on the membrane. The membrane was washed twice by adding 700 µl of buffer NT3 following 30 s centrifugation at 11 000 rcf. The membrane was dried by 1 min centrifugation at 11 000 rcf. The DNA was eluted into 40 µl of buffer NE and the DNA concentrations were determined using NanoDrop ND-1000 Spectrophotometer. 35 µl of the purified PCR product with DNA concentration between 10 and 40 ng/µl was sent for deep sequencing by the CRISPR Sequencing service from

Center for Computational and Integrative Biology DNA core of Massachusetts General Hospital (MGH CCIB DNA Core, 2023).

4.6 Data analysis

To determine nucleofection efficiency from bright-field and fluorescence cell images, ImageJ software was used to determine the total cell area and the area of cells expressing GFP. The deep sequencing data was processed using CRISPResso2 software (Clement et al., 2019). To assess whether the VAF data followed normal distribution, the results from D'Agnostino-Pearson test, Anderson-Darling test and Shapiro-Wilk test were compared. As the data did not follow normal distribution, the Wilcoxon signed-rank test was used to determine the difference in frameshift mutation allele frequencies between untreated and treated samples. A p-value below 0.05 was considered as a mark for statistically significant difference. The statistical testing was done, and all graphs were produced using GraphPad Prism version 10.2.0.

5 Acknowledgements

First and foremost, I would like to express my sincere gratitude to Kari Kurppa and Klaus Elenius for giving me the opportunity to conduct my master's thesis work in their research groups. I am especially grateful to my supervisor Kari Kurppa for all the guidance and encouragement during the thesis process. Furthermore, I want to extend my appreciation to all the members of Kurppa and Elenius research groups for creating such a great and welcoming working atmosphere, as well as for their assistance with various methodologies and techniques. Lastly, I am deeply thankful to my family for their encouragement and unwavering support throughout my whole studies.

6 List of abbreviations

ALK	anaplastic lymphoma kinase
CYT	cytoplasmic
EGFR	epidermal growth factor receptor
EML4	echinoderm microtubule-associated protein-like 4
ERBB	erythroblastic leukemia viral oncogene homolog
ERK	extracellular-signal-regulated kinase
HB-EGF	heparin-binding EGF-like growth factor
HER	human epidermal growth factor receptor
JM	juxtamembrane
MEK	mitogen-activated protein kinase/ERK kinase
NRG	neuregulin
NSCLC	non-small cell lung cancer
PI3K	phosphoinositide 3-kinase
PTK	protein tyrosine kinase
RTK	receptor tyrosine kinase
$s80^{HER4}$	intracellular domain of ERBB4
SOC	standard-of-care
TACE	tumor necrosis factor-α converting enzyme
TBST	tris-buffered saline with tween 20
TGF-α	transforming growth factor α
VAF	variant allele frequency

References

Abel, E. V., Basile, K. J., Kugel, C. H., Witkiewicz, A. K., Le, K., Amaravadi, R. K., Karakousis, G. C., Xu, X., Xu, W., Schuchter, L. M., Lee, J. B., Ertel, A., Fortina, P., & Aplin, A. E. (2013). Melanoma adapts to RAF/MEK inhibitors through FOXD3-mediated upregulation of ERBB3. *Journal of Clinical Investigation*, *123*(5), 2155–2168. https://doi.org/10.1172/JCI65780

Arteaga, C. L., & Engelman, J. A. (2014). ERBB receptors: From oncogene discovery to basic science to mechanism-based cancer therapeutics. *Cancer Cell*, *25*(3), 282–303. https://doi.org/10.1016/j.ccr.2014.02.025

Ascierto, P. A., Kirkwood, J. M., Grob, J.-J., Simeone, E., Grimaldi, A. M., Maio, M., Palmieri, G., Testori, A., Marincola, F. M., & Mozzillo, N. (2012). The role of BRAF V600 mutation in melanoma. *The Journal of Translational Medicine*, *10*(85). http://www.translational-medicine.com/content/10/1/85

Bio-Rad. (n.d.). *Mini Trans-Blot ® Electrophoretic Transfer Cell Instruction Manual*. Retrieved September 29, 2023, from https://www.bio-rad.com/sites/default/files/webroot/web/pdf/lsr/literature/M1703930.pdf

Bouffet, E., Hansford, J. R., Garrè, M. L., Hara, J., Plant-Fox, A., Aerts, I., Locatelli, F., van der Lugt, J., Papusha, L., Sahm, F., Tabori, U., Cohen, K. J., Packer, R. J., Witt, O., Sandalic, L., Bento Pereira da Silva, A., Russo, M., & Hargrave, D. R. (2023). Dabrafenib plus Trametinib in Pediatric Glioma with BRAF V600 Mutations . *New England Journal of Medicine*, *389*(12), 1108–1120. https://doi.org/10.1056/nejmoa2303815

Boumahdi, S., & de Sauvage, F. J. (2020). The great escape: tumour cell plasticity in resistance to targeted therapy. *Nature Reviews Drug Discovery*, *19*(1), 39–56. https://doi.org/10.1038/s41573-019-0044-1

Breuleux, M. (2007). Role of heregulin in human cancer. *Cellular and Molecular Life Sciences*, *64*(18), 2358–2377. https://doi.org/10.1007/s00018-007-7120-0

Burden, S., & Yarden, Y. (1997a). Neuregulins and Their Receptors: A Versatile Signaling Module in Organogenesis and Oncogenesis. *Neuron*, *18*(6), 847–855. https://doi.org/10.1016/S0896-6273(00)80324-4

Burden, S., & Yarden, Y. (1997b). Neuregulins and Their Receptors: Meeting Report A Versatile Signaling Module in Organogenesis and Oncogenesis. *Neuron*, *18*, 847–855.

Burgess, A. W., Cho, H.-S., Eigenbrot, C., Ferguson, K. M., Garrett, T. P. J., Leahy, D. J., Lemmon, M. A., Sliwkowski, M. X., Ward, C. W., & Yokoyama, S. (2003). An Open-and-Shut Case? Recent Insights into the Activation of EGF/ErbB Receptors. *Molecular Cell*, *12*, 541–552.

Cabanos, H. F., & Hata, A. N. (2021). Emerging insights into targeted therapy-tolerant persister cells in cancer. *Cancers*, *13*(11). https://doi.org/10.3390/cancers13112666

Cappuzzo, F., Marchetti, A., Skokan, M., Rossi, E., Gajapathy, S., Felicioni, L., Grammastro, M. Del, Sciarrotta, M. G., Buttitta, F., Incarbone, M., Toschi, L., Finocchiaro, G., Destro, A., Terracciano, L., Roncalli, M., Alloisio, M., Santoro, A., & Varella-Garcia, M. (2009). Increased MET gene copy number negatively affects survival of surgically resected non-small-cell lung cancer patients. *Journal of Clinical Oncology*, *27*(10), 1667–1674. https://doi.org/10.1200/JCO.2008.19.1635

Cheng, H., Terai, M., Kageyama, K., Ozaki, S., McCue, P. A., Sato, T., & Aplin, A. E. (2015). Paracrine effect of NRG1 and HGF drives resistance to MEK inhibitors in metastatic uveal melanoma. *Cancer Research*, *75*(13), 2737–2748. https://doi.org/10.1158/0008-5472.CAN-15-0370

Chong, C. R., & Jänne, P. A. (2013). The quest to overcome resistance to EGFR-targeted therapies in cancer. *Nature Medicine*, *19*(11), 1389–1400. https://doi.org/10.1038/nm.3388

Clement, K., Rees, H., Canver, M. C., Gehrke, J. M., Farouni, R., Hsu, J. Y., Cole, M. A., Liu, D. R., Joung, J. K., Bauer, D. E., & Pinello, L. (2019). CRISPResso2 provides accurate and rapid genome editing sequence analysis. *Nature Biotechnology*, *37*(3), 224–226. https://doi.org/10.1038/s41587-019-0032-3

Đorđević, M., Paunović, V., Jovanović Tucović, M., Tolić, A., Rajić, J., Dinić, S., Uskoković, A., Grdović, N., Mihailović, M., Marković, I., Arambašić Jovanović, J., & Vidaković, M. (2022). Nucleofection as an Efficient Method for Alpha TC1-6 Cell Line Transfection. *Applied Sciences (Switzerland)*, *12*(15). https://doi.org/10.3390/app12157938

Elenius, K., Choi, C. J., Paul, S., Santiestevan, E., Nishi, E., & Klagsbrun, M. (1999). Characterization of a naturally occurring ErbB4 isoform that does not bind or activate phosphatidyl inositol 3-kinase. *Oncogene*, *18*(24), 2607–2615. http://www.stockton-press.co.uk/onc

Erickson, S. L., O'Shea, K. S., Ghaboosi, N., Loverro, L., Frantz, G., Bauer, M., Lu, L. H., & Moore, M. W. (1997). ErbB3 is required for normal cerebellar and cardiac development: a comparison with ErbB2- and heregulin-deficient mice. *Development*, *124*(24), 4999–5011. https://doi.org/10.1242/dev.124.24.4999

Garrett, J. T., Olivares, M. G., Rinehart, C., Granja-Ingram, N. D., Sánchez, V., Chakrabarty, A., Dave, B., Cook, R. S., Pao, W., McKinely, E., Manning, H. C., Chang, J., & Arteaga, C. L. (2011). Transcriptional and posttranslational up-regulation of HER3 (ErbB3) compensates for inhibition of the HER2 tyrosine kinase. *Proceedings of the National Academy of Sciences of the United States of America*, *108*(12), 5021–5026. https://doi.org/10.1073/pnas.1016140108

Hata, A. N., Niederst, M. J., Archibald, H. L., Gomez-Caraballo, M., Siddiqui, F. M., Mulvey, H. E., Maruvka, Y. E., Ji, F., Bhang, H. E. C., Radhakrishna, V. K., Siravegna, G., Hu, H., Raoof, S., Lockerman, E., Kalsy, A., Lee, D., Keating, C. L., Ruddy, D. A., Damon, L. J., … Engelman, J. A. (2016). Tumor cells can follow distinct evolutionary paths to become resistant to epidermal growth factor receptor inhibition. *Nature Medicine*, *22*(3), 262–269. https://doi.org/10.1038/nm.4040

Hegde, G. V., De La Cruz, C. C., Chiu, C., Alag, N., Schaefer, G., Crocker, L., Ross, S., Goldenberg, D., Merchant, M., Tien, J., Shao, L., Roth, L., Tsai, S. P., Stawicki, S., Jin, Z., Wyatt, S. K., Carano, R. A. D., Zheng, Y., Sweet-Cordero, E. A., … Jackson, E. L. (2013). Blocking NRG1 and other ligand-mediated Her4 signaling enhances the magnitude and duration of the chemotherapeutic response of non-small cell lung cancer. *Science Translational Medicine*, *5*(171). https://doi.org/10.1126/scitranslmed.3004438

Horodecka, K., & Düchler, M. (2021). Crispr/cas9: Principle, applications, and delivery through extracellular vesicles. *International Journal of Molecular Sciences*, *22*(11). https://doi.org/10.3390/ijms22116072

Huang, L., Jiang, S., & Shi, Y. (2020). Tyrosine kinase inhibitors for solid tumors in the past 20 years (2001–2020). *Journal of Hematology and Oncology*, *13*(1). https://doi.org/10.1186/s13045-020-00977-0

Inamura, K., Takeuchi, K., Togashi, Y., Nomura, K., Ninomiya, H., Okui, M., Satoh, Y., Okumura, S., Nakagawa, K., Soda, M., Choi, Y. L., Niki, T., Mano, H., & Ishikawa, Y. (2008). EML4-ALK Fusion Is Linked to Histological Characteristics in a Subset of Lung Cancers. *Journal of Thoracic Oncology*, *3*(1), 13–17.

Katayama, R., Shaw, A. T., Khan, T. M., Mino-Kenudson, M., Solomon, B. J., Halmos, B., Jessop, N. A., Wain, J. C., Yeo, A. T., Benes, C., Drew, L., Saeh, J. C., Crosby, K., Sequist, L. V., Iafrate, A. J., & Engelman, J. A. (2012). Mechanisms of acquired crizotinib resistance in ALK-rearranged lung cancers. *Science Translational Medicine*, *4*(120). https://doi.org/10.1126/scitranslmed.3003316

Kim, J. Y., Jung, H. H., Do, I. G., Bae, S. Y., Lee, S. K., Kim, S. W., Lee, J. E., Nam, S. J., Ahn, J. S., Park, Y. H., & Im, Y. H. (2016). Prognostic value of ERBB4 expression in patients with triple negative breast cancer. *BMC Cancer*, *16*(1). https://doi.org/10.1186/s12885-016-2195-3

Kouranova, E., Forbes, K., Zhao, G., Warren, J., Bartels, A., Wu, Y., & Cui, X. (2016). CRISPRs for optimal targeting: Delivery of CRISPR components as DNA, RNA, and protein into cultured cells and single-cell embryos. *Human Gene Therapy*, *27*(6), 464–475. https://doi.org/10.1089/hum.2016.009

Kugel, C. H., Hartsough, E. J., Davies, M. A., Setiady, Y. Y., & Aplin, A. E. (2014). Function-blocking ERBB3 antibody inhibits the adaptive response to RAF inhibitor. *Cancer Research*, *74*(15), 4122–4132. https://doi.org/10.1158/0008-5472.CAN-14-0464

Lattanzi, A., Meneghini, V., Pavani, G., Amor, F., Ramadier, S., Felix, T., Antoniani, C., Masson, C., Alibeu, O., Lee, C., Porteus, M. H., Bao, G., Amendola, M., Mavilio, F., & Miccio, A. (2019). Optimization of CRISPR/Cas9 Delivery to Human Hematopoietic Stem and Progenitor Cells for

Therapeutic Genomic Rearrangements. *Molecular Therapy*, *27*(1), 137–150. https://doi.org/10.1016/j.ymthe.2018.10.008

Lax, I., Johnson, ' A, Howk, R., Sap, ' J, Bellot, F., Winkler, M., Ullrich, A., Vennstrom, B., Schlessinger, J., & Givollt, D. (1988). Chicken Epidermal Growth Factor (EGF) Receptor: cDNA Cloning, Expression in Mouse Cells, and Differential Binding of EGF and Transforming Growth Factor Alpha. *MOLECULAR AND CELLULAR BIOLOGY*, *8*(5), 1970–1978.

Lee, K.-F., Simon, H., Chen, H., Bates, B., Hung, M.-C., & Hauser, C. (1995). Requirement for neuregulin receptor erbB2 in neural and cardiac development. *Nature*, *378*(6555), 394–398. https://doi.org/10.1038/378394a0

Lemmon, M. A., Schlessinger, J., & Ferguson, K. M. (2014). The EGFR Family: Not So Prototypical Receptor Tyrosine Kinases. *Cold Spring Harbor Perspectives in Biology*, *6*(4), a020768–a020768. https://doi.org/10.1101/cshperspect.a020768

Loibl, S., & Gianni, L. (2017). HER2-positive breast cancer. *The Lancet*, *389*(10087), 2415–2429. https://doi.org/10.1016/S0140-6736(16)32417-5

Long, G. V., Stroyakovskiy, D., Gogas, H., Levchenko, E., de Braud, F., Larkin, J., Garbe, C., Jouary, T., Hauschild, A., Grob, J. J., Chiarion Sileni, V., Lebbe, C., Mandalà, M., Millward, M., Arance, A., Bondarenko, I., Haanen, J. B. A. G., Hansson, J., Utikal, J., … Flaherty, K. (2014). Combined BRAF and MEK Inhibition versus BRAF Inhibition Alone in Melanoma. *New England Journal of Medicine*, *371*(20), 1877–1888. https://doi.org/10.1056/nejmoa1406037

Määttä, J. A., Sundvall, M., Junttila, T. T., Peri, L., Laine, V. J. O., Isola, J., Egeblad, M., & Elenius, K. (2006). Proteolytic cleavage and phosphorylation of a tumor-associated ErbB4 isoform promote ligand-independent survival and cancer cell growth. *Molecular Biology of the Cell*, *17*(1), 67–79. https://doi.org/10.1091/mbc.E05-05-0402

Marine, J. C., Dawson, S. J., & Dawson, M. A. (2020). Non-genetic mechanisms of therapeutic resistance in cancer. *Nature Reviews Cancer*, *20*(12), 743–756. https://doi.org/10.1038/s41568-020-00302-4

Martínez-Jiménez, F., Muiños, F., Sentís, I., Deu-Pons, J., Reyes-Salazar, I., Arnedo-Pac, C., Mularoni, L., Pich, O., Bonet, J., Kranas, H., Gonzalez-Perez, A., & Lopez-Bigas, N. (2020). A compendium of mutational cancer driver genes. *Nature Reviews Cancer*, *20*(10), 555–572. https://doi.org/10.1038/s41568-020-0290-x

Mertens, F., Johansson, B., Fioretos, T., & Mitelman, F. (2015). The emerging complexity of gene fusions in cancer. *Nature Reviews Cancer*, *15*(6), 371–381. https://doi.org/10.1038/nrc3947

MGH CCIB DNA Core. (2023). *CRISPR Sequencing*. https://dnacore.mgh.harvard.edu/new-cgi-bin/site/pages/crispr_sequencing_main.jsp

Miele, E., Abballe, L., Spinelli, G. P., Besharat, Z. M., Catanzaro, G., Chiacchiarini, M., Vacca, A., Po, A., Capalbo, C., & Ferretti, E. (2020). BRAF mutant colorectal cancer: ErbB2 expression levels as predictive factor for the response to combined BRAF/ErbB inhibitors. *BMC Cancer*, *20*(1). https://doi.org/10.1186/s12885-020-6586-0

Miettinen, P. J., Berger, J. E., Meneses, J., Phung, Y., Pedersen, R. A., Werb, Z., & Derynck, R. (1995). Epithelial immaturity and multiorgan failure in mice lacking epidermal growth factor receptor. *Nature*, *376*(6538), 337–341. https://doi.org/10.1038/376337a0

Montero, J. C., Rodríguez-Barrueco, R., Ocaña, A., Díaz-Rodríguez, E., Esparís-Ogando, A., & Pandiella, A. (2008). Neuregulins and Cancer. *Clinical Cancer Research*, *14*(11), 3237–3241. https://doi.org/10.1158/1078-0432.CCR-07-5133

Montero, J. C., Rodríguez-Barrueco, R., Yuste, L., Juanes, P. P., Borges, J., Esparís-Ogando, A., & Pandiella, A. (2007). The Extracellular Linker of pro-Neuregulin-α2c Is Required for Efficient Sorting and Juxtacrine Function. *Molecular Biology of the Cell*, *18*(2), 380–393. https://doi.org/10.1091/mbc.e06-06-0511

Morris, V., Overman, M. J., Jiang, Z. Q., Garrett, C., Agarwal, S., Eng, C., Kee, B., Fogelman, D., Dasari, A., Wolff, R., Maru, D., & Kopetz, S. (2014). Progression-free survival remains poor over sequential lines of systemic therapy in patients with BRAF-mutated colorectal cancer. *Clinical Colorectal Cancer*, *13*(3), 164–171. https://doi.org/10.1016/j.clcc.2014.06.001

Muraoka-Cook, R. S., Sandahl, M. A., Strunk, K. E., Miraglia, L. C., Husted, C., Hunter, D. M., Elenius, K., Chodosh, L. A., & Earp, H. S. (2009). ErbB4 Splice Variants Cyt1 and Cyt2 Differ by 16 Amino Acids and Exert Opposing Effects on the Mammary Epithelium In Vivo. *Molecular and Cellular Biology*, *29*(18), 4935–4948. https://doi.org/10.1128/mcb.01705-08

Ni, C. Y., Murphy, M. P., Golde, T. E., & Carpenter, G. (2001). γ-secretase cleavage and nuclear locatization of ErbB-4 receptor tyrosine kinase. *Science*, *294*(5549), 2179–2181. https://doi.org/10.1126/science.1065412

Obenauf, A. C., Zou, Y., Ji, A. L., Vanharanta, S., Shu, W., Shi, H., Kong, X., Bosenberg, M. C., Wiesner, T., Rosen, N., Lo, R. S., & Massagué, J. (2015). Therapy-induced tumour secretomes promote resistance and tumour progression. *Nature*, *520*(7547), 368–372. https://doi.org/10.1038/nature14336

O'Bryant, C. L., Wenger, S. D., Kim, M., & Thompson, L. A. (2013). Crizotinib: A New Treatment Option for ALK-Positive Non-Small Cell Lung Cancer. *Annals of Pharmacotherapy*, *47*(2), 189–197. https://doi.org/10.1345/aph.1R002

Ochi, N., Takeyama, M., Miyake, N., Fuchigami, M., Yamane, H., Fukazawa, T., Nagasaki, Y., Kawahara, T., Nakanishi, H., & Takigawa, N. (2023). The complexity of EGFR exon 19 deletion and L858R mutant cells as assessed by proteomics, transcriptomics, and metabolomics. *Experimental Cell Research*, *424*(1). https://doi.org/10.1016/j.yexcr.2023.113503

Ogiso, H., Ishitani, R., Nureki, O., Fukai, S., Yamanaka, M., Kim, J.-H., Saito, K., Sakamoto, A., Inoue, M., Shirouzu, M., & Yokoyama, S. (2002). Crystal Structure of the Complex of Human Epidermal Growth Factor and Receptor Extracellular Domains. *Cell*, *110*, 775–787.

Passaro, A., Jänne, P. A., Mok, T., & Peters, S. (2021). Overcoming therapy resistance in EGFR-mutant lung cancer. *Nature Cancer*, *2*(4), 377–391. https://doi.org/10.1038/s43018-021-00195-8

Planchard, D., Besse, B., Groen, H. J. M., Souquet, P. J., Quoix, E., Baik, C. S., Barlesi, F., Kim, T. M., Mazieres, J., Novello, S., Rigas, J. R., Upalawanna, A., D'Amelio, A. M., Zhang, P., Mookerjee, B., & Johnson, B. E. (2016). Dabrafenib plus trametinib in patients with previously treated BRAFV600E-mutant metastatic non-small cell lung cancer: an open-label, multicentre phase 2 trial. *The Lancet Oncology*, *17*(7), 984–993. https://doi.org/10.1016/S1470-2045(16)30146-2

Prahallad, A., Sun, C., Huang, S., Di Nicolantonio, F., Salazar, R., Zecchin, D., Beijersbergen, R. L., Bardelli, A., & Bernards, R. (2012). Unresponsiveness of colon cancer to BRAF(V600E) inhibition through feedback activation of EGFR. *Nature*, *483*(7387), 100–104. https://doi.org/10.1038/nature10868

Prasetyanti, P. R., Capone, E., Barcaroli, D., D'Agostino, D., Volpe, S., Benfante, A., van Hooff, S., Iacobelli, V., Rossi, C., Iacobelli, S., Medema, J. P., De Laurenzi, V., & Sala, G. (2015). ErbB-3 activation by NRG-1β sustains growth and promotes vemurafenib resistance in BRAF-V600E colon cancer stem cells (CSCs). *Oncotarget*, *6*(19), 16902–16911. https://doi.org/10.18632/oncotarget.4642

Remon, J., Hendriks, L. E. L., Mountzios, G., García-Campelo, R., Saw, S. P. L., Uprety, D., Recondo, G., Villacampa, G., & Reck, M. (2023). MET alterations in NSCLC—Current Perspectives and Future Challenges. *Journal of Thoracic Oncology*, *18*(4), 419–435. https://doi.org/10.1016/j.jtho.2022.10.015

Santarius, T., Shipley, J., Brewer, D., Stratton, M. R., & Cooper, C. S. (2010). A census of amplified and overexpressed human cancer genes. *Nature Reviews Cancer*, *10*(1), 59–64. https://doi.org/10.1038/nrc2771

Segers, V. F. M., Dugaucquier, L., Feyen, E., Shakeri, H., & De Keulenaer, G. W. (2020). The role of ErbB4 in cancer. *Cellular Oncology*, *43*(3), 335–352. https://doi.org/10.1007/s13402-020-00499-4

Shaffer, S. M., Dunagin, M. C., Torborg, S. R., Torre, E. A., Emert, B., Krepler, C., Beqiri, M., Sproesser, K., Brafford, P. A., Xiao, M., Eggan, E., Anastopoulos, I. N., Vargas-Garcia, C. A., Singh, A., Nathanson, K. L., Herlyn, M., & Raj, A. (2017). Rare cell variability and drug-induced reprogramming as a mode of cancer drug resistance. *Nature*, *546*(7658), 431–435. https://doi.org/10.1038/nature22794

Sharma, S. V., Lee, D. Y., Li, B., Quinlan, M. P., Takahashi, F., Maheswaran, S., McDermott, U., Azizian, N., Zou, L., Fischbach, M. A., Wong, K. K., Brandstetter, K., Wittner, B., Ramaswamy, S., Classon, M., & Settleman, J. (2010). A Chromatin-Mediated Reversible Drug-Tolerant State in Cancer Cell Subpopulations. *Cell*, *141*(1), 69–80. https://doi.org/10.1016/j.cell.2010.02.027

Shen, S., Vagner, S., & Robert, C. (2020). Persistent Cancer Cells: The Deadly Survivors. *Cell*, *183*(4), 860–874. https://doi.org/10.1016/j.cell.2020.10.027

Slamon, D. J., Clark, G. M., Wong, S. G., Levin, W. J., Ullrich, A., & Mcguire, W. L. (1987). Human Breast Cancer: Correlation of Relapse and Survival with Amplification of the HER-2/neu Oncogene. *Science*, *235*, 177–182. https://www.science.org

Soda, M., Choi, Y. L., Enomoto, M., Takada, S., Yamashita, Y., Ishikawa, S., Fujiwara, S. I., Watanabe, H., Kurashina, K., Hatanaka, H., Bando, M., Ohno, S., Ishikawa, Y., Aburatani, H., Niki, T., Sohara, Y., Sugiyama, Y., & Mano, H. (2007). Identification of the transforming EML4-ALK fusion gene in non-small-cell lung cancer. *Nature*, *448*(7153), 561–566. https://doi.org/10.1038/nature05945

Stratton, M. R., Campbell, P. J., & Futreal, P. A. (2009). The cancer genome. *Nature*, *458*(7239), 719–724. https://doi.org/10.1038/nature07943

Subbiah, V., Kreitman, R. J., Wainberg, Z. A., Cho, J. Y., Schellens, J. H. M., Soria, J. C., Wen, P. Y., Zielinski, C. C., Cabanillas, M. E., Boran, A., Ilankumaran, P., Burgess, P., Romero Salas, T., & Keam, B. (2022). Dabrafenib plus trametinib in patients with BRAF V600E-mutant anaplastic thyroid cancer: updated analysis from the phase II ROAR basket study. *Annals of Oncology*, *33*(4), 406–415. https://doi.org/10.1016/j.annonc.2021.12.014

Subbiah, V., Lassen, U., Élez, E., Italiano, A., Curigliano, G., Javle, M., de Braud, F., Prager, G. W., Greil, R., Stein, A., Fasolo, A., Schellens, J. H. M., Wen, P. Y., Viele, K., Boran, A. D., Gasal, E., Burgess, P., Ilankumaran, P., & Wainberg, Z. A. (2020). Dabrafenib plus trametinib in patients with BRAFV600E-mutated biliary tract cancer (ROAR): a phase 2, open-label, single-arm, multicentre basket trial. *The Lancet Oncology*, *21*(9), 1234–1243. https://doi.org/10.1016/S1470-2045(20)30321-1

Suda, K., Onozato, R., Yatabe, Y., & Mitsudomi, T. (2009). EGFR T790M mutation: A double role in lung cancer cell survival? *Journal of Thoracic Oncology*, *4*(1), 1–4. https://doi.org/10.1097/JTO.0b013e3181913c9f

Sung, H., Ferlay, J., Siegel, R. L., Laversanne, M., Soerjomataram, I., Jemal, A., & Bray, F. (2021). Global Cancer Statistics 2020: GLOBOCAN Estimates of Incidence and Mortality Worldwide for 36 Cancers in 185 Countries. *CA: A Cancer Journal for Clinicians*, *71*(3), 209–249. https://doi.org/10.3322/caac.21660

Suo, Z., Risberg, B., Kalsson, M. G., Willman, K., Tierens, A., Skovlund, E., & Nesland, J. M. (2002). EGFR family expression in breast carcinomas c-erbB-2 and c-erbB-4 receptors have different effects on survival. *Journal of Pathology*, *196*(1), 17–25. https://doi.org/10.1002/path.1003

Takala, I. (2022). *Non-genetic rewiring of ERBB signaling in cancer drug tolerance* [Master's thesis]. University of Turku.

Tanizaki, J., Okamoto, I., Okabe, T., Sakai, K., Tanaka, K., Hayashi, H., Kaneda, H., Takezawa, K., Kuwata, K., Yamaguchi, H., Hatashita, E., Nishio, K., & Nakagawa, K. (2012). Activation of

HER family signaling as a mechanism of acquired resistance to ALK inhibitors in EML4-ALK-positive non-small cell lung cancer. *Clinical Cancer Research*, *18*(22), 6219–6226. https://doi.org/10.1158/1078-0432.CCR-12-0392

Thybusch-Bernhardt, A., Beckmann, S., & Juhl, H. (2001). Comparative analysis of the EGF-receptor family in pancreatic cancer: expression of HER-4 correlates with a favourable tumor stage. *International Journal of Surgical Investigation*, *2*(5), 393–400.

Turk, R., & Spencer, N. Y. (2019, July 2). *Similar editing efficiency with two-part and single guide RNA*. Integrated DNA Technologies. https://www.idtdna.com/pages/education/decoded/article/a-high-degree-of-similarity-in-crispr-cas9-editing-efficiency-is-found-between-2-part-guide-rnas-and-single-guide-rnas

Veikkolainen, V., Vaparanta, K., Halkilahti, K., Iljin, K., Sundvall, M., & Elenius, K. (2011). Function of ERBB4 is determined by alternative splicing. *Cell Cycle*, *10*(16), 2647–2657. https://doi.org/10.4161/cc.10.16.17194

Vidal, G. A., Clark, D. E., Marrero, L., & Jones, F. E. (2007). A constitutively active ERBB4/HER4 allele with enhanced transcriptional coactivation and cell-killing activities. *Oncogene*, *26*(3), 462–466. https://doi.org/10.1038/sj.onc.1209794

Wali, V. B., Gilmore-Hebert, M., Mamillapalli, R., Haskins, J. W., Kurppa, K. J., Elenius, K., Booth, C. J., & Stern, D. F. (2014). Overexpression of ERBB4 JM-a CYT-1 and CYT-2 isoforms in transgenic mice reveals isoformspecific roles in mammary gland development and carcinogenesis. *Breast Cancer Research*, *16*(1). https://doi.org/10.1186/s13058-014-0501-z

Wang, S. W., Gao, C., Zheng, Y. M., Yi, L., Lu, J. C., Huang, X. Y., Cai, J. Bin, Zhang, P. F., Cui, Y. H., & Ke, A. W. (2022). Current applications and future perspective of CRISPR/Cas9 gene editing in cancer. *Molecular Cancer*, *21*(1). https://doi.org/10.1186/s12943-022-01518-8

Wege, A. K., Chittka, D., Buchholz, S., Klinkhammer-Schalke, M., Diermeier-Daucher, S., Zeman, F., Ortmann, O., & Brockhoff, G. (2018). HER4 expression in estrogen receptor-positive breast cancer is associated with decreased sensitivity to tamoxifen treatment and reduced overall survival of postmenopausal women. *Breast Cancer Research*, *20*(1). https://doi.org/10.1186/s13058-018-1072-1

Weinstein, I. B. (2002). Cancer: Addiction to oncogenes - The Achilles heal of cancer. *Science*, *297*(5578), 63–64. https://doi.org/10.1126/science.1073096

Williams, C. S., Bernard, J. K., Beckler, M. D., Almohazey, D., Washington, M. K., Smith, J. J., & Frey, M. R. (2015). ERBB4 is over-expressed in human colon cancer and enhances cellular transformation. *Carcinogenesis*, *36*(7), 710–718. https://doi.org/10.1093/carcin/bgv049

Wilson, F. H., Johannessen, C. M., Piccioni, F., Tamayo, P., Kim, J. W., VanAllen, E. M., Corsello, S. M., Capelletti, M., Calles, A., Butaney, M., Sharifnia, T., Gabriel, S. B., Mesirov, J. P., Hahn, W. C., Engelman, J. A., Meyerson, M., Root, D. E., Jänne, P. A., & Garraway, L. A. (2015). A

Functional Landscape of Resistance to ALK Inhibition in Lung Cancer. *Cancer Cell*, *27*(3), 397–408. https://doi.org/10.1016/j.ccell.2015.02.005

Wilson, T. R., Fridlyand, J., Yan, Y., Penuel, E., Burton, L., Chan, E., Peng, J., Lin, E., Wang, Y., Sosman, J., Ribas, A., Li, J., Moffat, J., Sutherlin, D. P., Koeppen, H., Merchant, M., Neve, R., & Settleman, J. (2012). Widespread potential for growth-factor-driven resistance to anticancer kinase inhibitors. *Nature*, *487*(7408), 505–509. https://doi.org/10.1038/nature11249

World Health Organization (WHO). (2020). *Global Health Estimates 2020: Deaths by Cause, Age, Sex, by Country and by Region, 2000-2019*. who.int/ data/gho/data/theme s/morta lity-and globa l-healt h-estim ates/ghe-leadi ng causes-of-death

Wu, P., Nielsen, T. E., & Clausen, M. H. (2015). FDA-approved small-molecule kinase inhibitors. *Trends in Pharmacological Sciences*, *36*(7), 422–439. https://doi.org/10.1016/j.tips.2015.04.005

Yamada, T., Takeuchi, S., Nakade, J., Kita, K., Nakagawa, T., Nanjo, S., Nakamura, T., Matsumoto, K., Soda, M., Mano, H., Uenaka, T., & Yano, S. (2012). Paracrine receptor activation by microenvironment triggers bypass survival signals and ALK inhibitor resistance in EML4-ALK lung cancer cells. *Clinical Cancer Research*, *18*(13), 3592–3602. https://doi.org/10.1158/1078-0432.CCR-11-2972

Yamaguchi, N., Lucena-Araujo, A. R., Nakayama, S., de Figueiredo-Pontes, L. L., Gonzalez, D. A., Yasuda, H., Kobayashi, S., & Costa, D. B. (2014). Dual ALK and EGFR inhibition targets a mechanism of acquired resistance to the tyrosine kinase inhibitor crizotinib in ALK rearranged lung cancer. *Lung Cancer*, *83*(1), 37–43. https://doi.org/10.1016/j.lungcan.2013.09.019

Yang, H., Jiang, D., Li, W., Liang, J., Gentry, L. E., & Brattain, M. G. (2000). Defective cleavage of membrane bound TGFα leads to enhanced activation of the EGF receptor in malignant cells. *Oncogene*, *19*(15), 1901–1914. https://doi.org/10.1038/sj.onc.1203513

Yang, L., Li, Y., Shen, E., Cao, F., Li, L., Li, X., Wang, X., Kariminia, S., Chang, B., Li, H., & Li, Q. (2017). NRG1-dependent activation of HER3 induces primary resistance to trastuzumab in HER2-overexpressing breast cancer cells. *International Journal of Oncology*, *51*(5), 1553–1562. https://doi.org/10.3892/ijo.2017.4130

Yang, Y., Li, S., Wang, Y., Zhao, Y., & Li, Q. (2022). Protein tyrosine kinase inhibitor resistance in malignant tumors: molecular mechanisms and future perspective. *Signal Transduction and Targeted Therapy*, *7*(1). https://doi.org/10.1038/s41392-022-01168-8

Yarden, Y., & Pines, G. (2012). The ERBB network: At last, cancer therapy meets systems biology. *Nature Reviews Cancer*, *12*(8), 553–563. https://doi.org/10.1038/nrc3309

Yarden, Y., & Sliwkowski, M. X. (2001). Untangling the ErbB signaling network. *Nature Reviews Molecular Cell Biology*, *2*. https://doi.org/10.1038/35052073

Yun, C. H., Boggon, T. J., Li, Y., Woo, M. S., Greulich, H., Meyerson, M., & Eck, M. J. (2007). Structures of Lung Cancer-Derived EGFR Mutants and Inhibitor Complexes: Mechanism of

Activation and Insights into Differential Inhibitor Sensitivity. *Cancer Cell*, *11*(3), 217–227. https://doi.org/10.1016/j.ccr.2006.12.017

Yun, C.-H., Mengwasser, K. E., Toms, A. V, Woo, M. S., Greulich, H., Wong, K.-K., Meyerson, M., & Eck, M. J. (2007). The T790M mutation in EGFR kinase causes drug resistance by increasing the affinity for ATP. *Proceedings of the National Academy of Sciences*. www.pnas.org/cgi/content/full/

Appendices

Appendix 1 - Preparation of buffers for western blotting

Lysis buffer

Amounts for preparation of 20 ml of lysis buffer used for preparation of samples for western blotting. Lysis stock containing all the components except the protease and phosphatase inhibitor cocktail was prepared and stored at 4 ℃. The protease and phosphatase inhibitor cocktail was added separately to the used volume of lysis stock each time before adding the lysis buffer to the cells.

Component	**Amount**
NP-40/Triton X-100	200 µl
1 M Tris-Cl pH 7.4	200 µl
0.5 M EDTA	40 µl
1 M NaF	200 µl
MQ water	19.36 ml
100X Halt™ Protease and Phosphatase Inhibitor Cocktail (Thermo Fisher Scientific, cat. no. 78440)	1:100 dilution

6x SDS sample buffer

Components for preparation of 6x SDS sample buffer.

Component	**Amount**
4x Tris-Cl/SDS pH 6.8	7 ml
Glycerol	3 ml
SDS	1 g
DTT	0.93 g
Bromphenol blue	1.2 mg

10x Western buffer

Components for preparation of 2 L of 10x western buffer, which was used for preparation of SDS-page running buffer and transfer buffer.

Component	**Amount**
Tris	60.4 g
Glycine	288 g
MQ water	2 L

Running buffer

Components for preparation of 5 L of SDS-page running buffer.

Component	Amount
10x western buffer	500 ml
SDS	5 g
MQ water	4.5 L

Transfer buffer

Components for preparation of 5 L of transfer buffer.

Component	Amount
10x western buffer	500 ml
Methanol	1 L
MQ water	3.5 L

Stripping buffer

Components for preparation of 2 L of stripping buffer.

Component	Amount
Glycine	15.01 g
HCl	10 ml
MQ water	2 L

10x TBST

Components for preparation of 2 L of 10x TBST. The 10x buffer was diluted 1:10 in MQ water before use.

Component	Amount
NaCl	176 g
Tween20	10 ml
1 M Tris-HCl pH 7.5	200 ml
MQ water	1.8 L

Appendix 2 - crRNA sequences

Sequences of crRNAs used for knocking out ERBB receptors by CRISPR-Cas9. The crRNAs were ordered from IDT.

crRNA name	Sequence
Hs.Cas9.EGFR.1.AA	TGCTGACTATGTCCCGCCAC
Hs.Cas9.EGFR.1.AC	GAGTAACAAGCTCACGCAGT
Hs.Cas9.ERBB2.1.AB	GCCCTTACACATCGGAGAAC
Hs.Cas9.ERBB2.1.AC	GATAGACACCAACCGCTCTC
Hs.Cas9.ERBB3.1.AA	GAGGGACCCAGGTCTACGAT
Hs.Cas9.ERBB3.1.AB	CACTGTACAAGCTCTACGAG
Hs.Cas9.ERBB4.1.AA	CGTTGCCATAAGTCCTGTAC
Hs.Cas9.ERBB4.1.AB	AGTCACAGGCTACGTGTTAG

Appendix 3 - PCR primer sequences

Nucleotide sequences, Tm values and GC content of DNA primers used for amplifying regions of genomic DNA targeted by CRISPR-Cas9. The annealing temperature for each primer pair is included.

Primer name	Nucleotide sequence	Tm	GC content	Annealing temperature
EGFR_AA_fwd	ATGCGAAGAGCACATGCATC	61 ℃	50 %	63 ℃
EGFR_AA_rev	TATGCGACACTTACAGCTGC	60 ℃	50 %	
ERBB2_AB_fwd	TGTTACTAACCCGTCCTCTC	58 ℃	50 %	61 ℃
ERBB2_AB_rev	CCTGTATGACACCTGCATTC	58 ℃	50 %	
ERBB3_AA_fwd	TGACAGGCTATGTCCTCGTG	61 ℃	55 %	64 ℃
ERBB3_AA_rev	TACCAGTCTTGGGCTGGCTG	64 ℃	60 %	
ERBB4_AA_fwd	GATGACCAGAGGCATGAAATG	59 ℃	48 %	61 ℃
ERBB4_AA_rev	CTCCTAGTCAAGGAGTGAAAG	57 ℃	48 %	